

NASA TECHNICAL NOTE



NASA TN D-3112

NASA TN D-3112

FACILITY FORM 602

N 66-12154	
(ACCESSION NUMBER)	(THRU)
54	1
(PAGES)	(CODE)
	30
(NASA CR OR TMX OR AD NUMBER)	(CATEGORY)

GPO PRICE \$ _____

CFSTI PRICE(S) \$ 3.00

Hard copy (HC) _____

Microfiche (MF) .50

ff 653 July 65

**A STUDY OF GEMINI-AGENA DOCKING
 USING A FIXED-BASE SIMULATOR
 EMPLOYING A CLOSED-CIRCUIT
 TELEVISION SYSTEM**

*by Donald R. Riley, Byron M. Jaquet, Richard E. Bardusch,
 and Perry L. Deal*

*Langley Research Center
 Langley Station, Hampton, Va.*

A STUDY OF GEMINI-AGENA DOCKING
USING A FIXED-BASE SIMULATOR EMPLOYING A
CLOSED-CIRCUIT TELEVISION SYSTEM

By Donald R. Riley, Byron M. Jaquet, Richard E. Bardusch,
and Perry L. Deal

Langley Research Center
Langley Station, Hampton, Va.

NATIONAL AERONAUTICS AND SPACE ADMINISTRATION

For sale by the Clearinghouse for Federal Scientific and Technical Information
Springfield, Virginia 22151 - Price \$3.00

A STUDY OF GEMINI-AGENA DOCKING
USING A FIXED-BASE SIMULATOR EMPLOYING A
CLOSED-CIRCUIT TELEVISION SYSTEM

By Donald R. Riley, Byron M. Jaquet, Richard E. Bardusch,
and Perry L. Deal
Langley Research Center

SUMMARY

12154

A full-size Gemini-Agena docking study was made using a visual docking simulator to determine some of the effects on docking of spacecraft attitude control mode, control power, target lighting, and target oscillatory motion. Flights were initiated at a range of about 300 feet (91.44 m) and were made using only visual observation of the target for guidance information. The results indicate that the spacecraft rate-command attitude control mode (primary) was well suited to the docking task. Consistent within-tolerance dockings could be obtained with the direct attitude control mode (backup), but the task was difficult and required considerable practice to become proficient. Design thrust levels for translation and attitude control jets permitted satisfactory docking operations; however, in a limited study using one research pilot one-half design thruster outputs were preferred for close-in maneuvering. Performance degradations for darkside dockings were obtained when only the docking ring was illuminated. With the addition of visual aids to provide boresight information, results comparable to daytime flights were obtained. The effects of target sinusoidal yawing oscillations on docking for motion amplitudes of $\pm 1^\circ$ and $\pm 2.5^\circ$ and oscillation periods from 60 to 10 seconds were negligible. For target amplitudes of $\pm 5^\circ$, degradations in docking performance as a function of period for periods less than 60 seconds were evident.

Becker

INTRODUCTION

One of the primary missions of the Gemini program is to demonstrate the ability of human pilots to perform the docking of two vehicles in space. Accomplishment of this task will help insure success of the lunar-orbit-rendezvous technique for exploration of the moon and other manned space missions as well.

Prior to actual space-flight docking, ground-based simulators will be used to explore the wide range of operational situations that the astronauts could encounter. A number of initial simulator studies (refs. 1 to 4, for example) illustrated the feasibility of pilot-controlled docking. In addition to general studies, a number of specific simulations employing Gemini-Agena design

characteristics have been undertaken. Simulations involving fixed- and moving-base simulators have been employed at the Langley Research Center. References 5, 6, and 7 provide some of the results of these studies.

The purpose of the present paper is to present the results of the fixed-base simulation studies of pilot-controlled Gemini-Agena docking made at the NASA Langley Research Center. Those portions of the investigation not previously reported are emphasized. The effects of attitude control mode, either rate command (primary) or direct acceleration command (backup), on docking as well as the effects of control power, target lighting, and single-degree-of-freedom target oscillations were investigated. The fixed-base simulator employed closed-circuit TV to provide a full-size out-of-the-window view of the Agena target vehicle. All docking flights were made using only pilot observation of the target through the spacecraft window for guidance information. Performance data, terminal conditions, and pilot ratings for docking flights initiated at a range of about 300 feet (91.44 m) for the paraglider configuration of the Gemini spacecraft are presented.

SYMBOLS

Both the U.S. Customary Units and the International System of Units (SI) are employed herein. Factors relating these two systems are given in reference 8.

The system of axes employed for the present study is shown in figure 1 and the symbols used are defined as follows:

F_X, F_Y, F_Z	total forces in the direction of the X, Y, and Z reference axes, respectively, lb (N)
$F_{X,b}, F_{Y,b}, F_{Z,b}$	total forces along Gemini body axes produced by translation and attitude-control reaction jets, lb (N)
$I_{X,b}, I_{Y,b}, I_{Z,b}$	moments of inertia about Gemini body axes, slug-ft ² (kg-m ²)
$I_{XZ,b}, I_{YZ,b}, I_{XY,b}$	products of inertia about Gemini body axes, slug-ft ² (kg-m ²)
I_{sp}	specific impulse, sec
$M_{X,b}, M_{Y,b}, M_{Z,b}$	moments produced about Gemini body axes by translation and attitude-control reaction jets, ft-lb (J)
T/m	ratio of translational jet thrust to vehicle mass, ft/sec ² (m/s ²)
m	Gemini mass, slugs (kg)

p, q, r	angular rates about Gemini body axes, rad/sec or deg/sec
P	period of target oscillation, sec
Δt_n	time for a given control input, sec
t	time, sec
X, Y, Z	right-handed system of reference axes with origin located at center of gravity of Agena vehicle (see fig. 1) and with X- and Z-axes in orbital plane
X_b, Y_b, Z_b	right-handed system of body axes with origin located at Gemini center of gravity
X_t, Y_t, Z_t	right-handed system of body axes with origin located at Agena center of gravity
x, y, z	distances along X-, Y-, and Z-axes, respectively, ft (m)
ψ, θ, ϕ	Euler angles in specified order relating position of Gemini body axes and reference axes, deg or rad (see fig. 1)
ψ_t	instantaneous target angle of yaw relative to X, Y, and Z reference axes, deg or rad
$\psi_{t, \max}$	maximum amplitude of target yawing oscillatory motion, deg or rad
ω	rate of rotation of reference axis system about earth at an altitude of 150 nautical miles (277.8 km), 0.0012 rad/sec
ϵ	rate command system error signal defined as difference between commanded and actual spacecraft angular rate (see sketch 2), deg/sec or rad/sec

- Notes: (1) One dot over a symbol denotes the first derivative with respect to time.
- (2) Two dots over a symbol denote the second derivative with respect to time.
- (3) Displacements and velocities with subscript "nose" indicate relative conditions at contact between spacecraft nose and center of docking ring in target reference frame of axes.

DESCRIPTION OF GEMINI AND AGENA VEHICLES

Gemini Spacecraft

The Gemini vehicle is a second-generation manned spacecraft designed for a two-man crew. An artist's sketch of the vehicle nearing completion of the docking maneuver is shown in figure 2. The spacecraft consists of two units, a reentry vehicle and a maneuvering module, that are joined together at about the heat-shield location. The propulsion system used to control orbital flight, rendezvous, and docking is contained within the maneuvering module. (See fig. 3.) There are eight attitude control jets and eight translation jets, all of which use hypergolic fuel. Of the eight attitude jets, four are primarily for pitch and four primarily for yaw. Roll can be obtained using either the pitch or the yaw jets at the option of the pilot by means of a selector switch on the control panel. For translation, pairs of jets provide fore and aft movement of the spacecraft, whereas single jets provide vertical and lateral maneuvering. All 16 jets are located rearward of the spacecraft's center of gravity. Because of this rearward location, strong coupling occurs between vertical and lateral control inputs and the pitch and yaw spacecraft motions. Similarly, pitch and yaw control inputs introduce vertical and lateral translations. Additional coupling, such as roll coupling with lateral translation inputs due to the presence of jet misalignments or center-of-gravity travel, can also be present but is of smaller magnitude.

For docking, two attitude control modes are available in the spacecraft. The primary mode is rate command in which a deflection of the hand controller commands an angular rate proportional to controller deflection. The presence of rate feedback in the system compensates for the coupling of the translation control inputs into the angular motions. The backup mode is a direct on-off acceleration command system in which deflection of the hand controller actuates a microswitch that commands full thrust from the attitude control jets. With this mode the pilot must provide manually the corrections necessary to account for the control coupling effects. With both attitude modes, on-off acceleration control is used for translation.

Agema Vehicle

The Agema target vehicle (fig. 2) has a 5-foot-diameter (1.52 m) docking ring that is shock mounted to absorb the impact forces at vehicle contact. The inner surface of the docking ring is conical in shape and serves to channel the Gemini nose to the latching position. The V-shaped slot in the docking ring and the indexing bar on the Gemini provide the necessary roll alignment for the latching mechanism.

SIMULATION

Simulator

An isometric sketch of the visual docking simulator used herein is presented as figure 4. This simulator is of the fixed-base type and consists of general-purpose analog-computer equipment combined with a U.S. Air Force aerial gunnery trainer, type F-151, that had been modified for the docking study. A full-scale wooden mockup of the Gemini vehicle is mounted within a 20-foot-diameter (6.10 m) spherical projection screen. The display system in the gunnery trainer included a closed-circuit television system. A small-scale model of the Agena target vehicle was mounted in a gimbal mechanism in front of the television camera (fig. 5). The model translates along the camera axis and rotates in three degrees of freedom. The camera video signal is transmitted to the projection system mounted vertically above the pilot (fig. 6). The image of the target is projected on a flat front-surfaced mirror that is servo driven about two axes and located at the center of the sphere a short distance above the pilot's head. The mirror positions the target image on the screen at the appropriate azimuth and elevation angles for the pilot's line of sight. A full six-degree-of-freedom motion is simulated by means of the model and mirror movements. Pilot control signals are sent to the analog computer, which solves the equations of relative motion between the spacecraft and target. The computer outputs are converted in the gunnery trainer to line-of-sight range, target angular aspect about the line of sight, and spatial location. These signals are used to drive the appropriate servomechanisms to provide the proper image and position for display to the pilot. The operating volume of the simulator permitted translational maneuvers up to a maximum displacement of 300 feet (91.44 m) longitudinally and ± 150 feet (45.72 m) laterally and vertically.

The Agena model was mounted at its midpoint in a three-axis gimbal box. For this study, the center of gravity of the Agena was assumed to coincide with this mounting point. The model markings used in the simulation are shown in figure 7 and were employed to provide some contrast in the visual display between the docking ring and recessed booster casing to aid in vehicle alignment. These markings are not employed on the actual Agena vehicle.

The pilot and observer (when present) were seated vertically in the simulator for comfort in a 1 g field. In the actual Gemini spacecraft, both astronauts are inclined from the longitudinal plane of symmetry of the spacecraft. Because the TV visual display is correctly projected only for the pilot, the simulator was arranged to be flown only from the left-hand seat, which is the command astronaut's position in the actual Gemini spacecraft. With the pilot's spine vertical, the eyes were located at the proper position with respect to the window. The hand controllers employed were oriented with respect to the pilot's seat.

It should be noted that the longitudinal distance between the eyes and the indexing bar (considered to be on the Gemini nose for the simulation) was 9.73 feet (2.97 m). This distance is greater than that for the actual Gemini spacecraft. The index bar was placed against the 10-foot-radius (3.05 m) spherical projection screen in order to avoid complicated parallax problems.

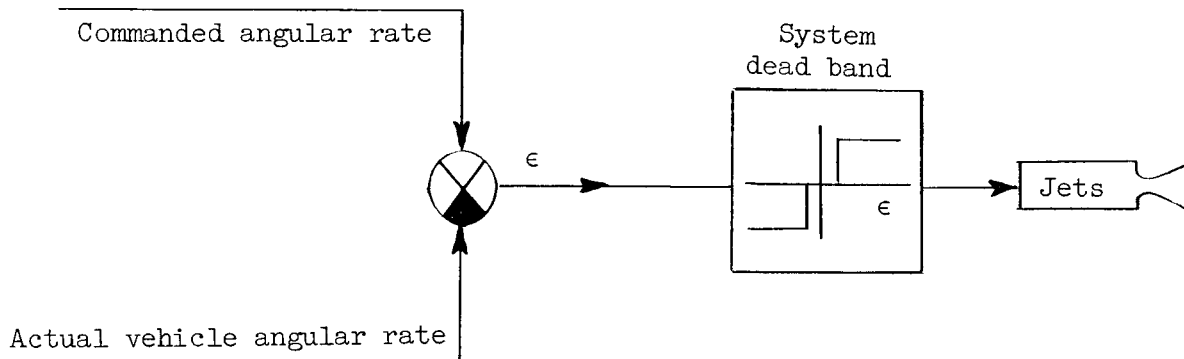
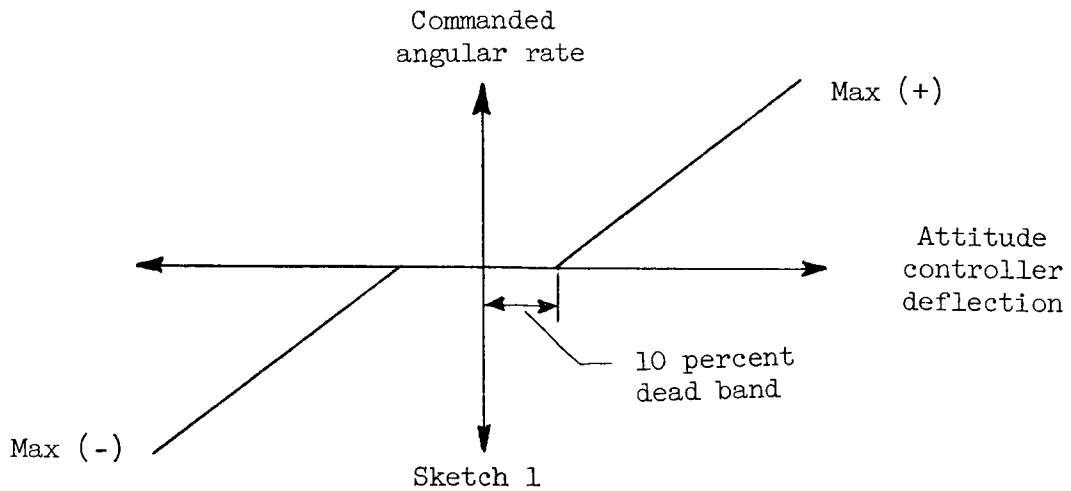
A random star background was provided as part of the visual display at various times during the investigation. The star projector was mounted in a gimbal arrangement that provided three angular degrees of freedom about its center and was located above the pilot's head next to the front-surfaced mirror (fig. 6).

Gemini Control Characteristics

Translational and rotational motions of the manned spacecraft were assumed to be produced by the reaction jets shown in figure 3. The design thrust levels of 100 pounds (444.82 N) for each translation jet and 25 pounds (111.21 N) for each attitude jet were employed. Time lags for these jets were not considered. Spacecraft control was commanded by the pilot using the three-axis finger-tip controllers shown in figure 8. Translational control was obtained using the left-hand controller, whereas vehicle attitude was controlled using the right-hand controller. These controllers are not prototype Gemini hand controllers. Prototype hand controllers were installed in the simulator for a later research program. (See ref. 9.) The instruments shown on the panel in figure 8 displayed spacecraft attitudes, angular rates, range, and range-rate information. The instruments were used for simulator checkout and initial pilot familiarization and then were covered for the test program.

The translation controller was an on-off spring centered device by which maximum thrust was commanded from the appropriate reaction jets when the corresponding controller deflection exceeded about $3/8$ inch (0.95 cm). Construction of the device permitted commands to be applied along each of the three vehicle axes individually or simultaneously simply by deflection of the controller in the direction of the desired motion of the spacecraft. A visual indication that the reaction jets were firing was supplied to the pilot by means of three dim red indicator lights (one light for each axis) arranged horizontally and located on the lower left side of the instrument panel.

The attitude controller, also a spring centered device, had a maximum controller deflection about each axis of approximately 30° . Single axis or combined inputs could be employed. No visual indication similar to the translation system was provided. A selector switch on the instrument panel dictated whether the attitude controller was commanding in the rate-command (primary) or direct (backup) control mode. In the rate-command mode, maximum vehicle rates of $\pm 8^\circ$ per second in roll and $\pm 4^\circ$ per second in pitch and yaw could be obtained by deflecting the hand controller to the maximum position about the appropriate axis. The rate-command system operated outside a dead band of 0.1° per second about all three axes. The rate-command system is described in the following two sketches:



The rate-command mode used in the simulation differed from that provided in the actual spacecraft as shown in the following table:

	Simulation	Spacecraft
Maximum roll rate, deg/sec	±8	±15
Maximum pitch rate, deg/sec	±4	±10
Maximum yaw rate, deg/sec	±4	±10
System dead band, deg/sec	±0.1	±0.2

The direct attitude control mode was an on-off acceleration command system providing maximum thrust from the reaction jets when the controller deflection exceeded the 10-percent dead band.

EQUATIONS OF MOTION

Six-degree-of-freedom equations of relative motion between the Agena target vehicle and the Gemini spacecraft were used in the simulation. These equations

were solved on an electronic analog computer operating in real time. The pilot closed the loop and had direct input into all six equations. The equations used are presented in appendix A.

PILOT'S TASK

The pilot flew from the left-hand seat, and his task was to take control of the Gemini from the initial conditions and to maneuver the vehicle until it began to enter the Agena docking ring within specified design tolerances. Only out-of-the-window observation of the target was used for guidance information. The pilot was permitted to use whatever technique he preferred to accomplish the task with no restraints on fuel and flight time.

In order to achieve successful docking, the pilot was required to position the center of the Gemini nose within ± 1 foot (0.30 m) of the center of the docking ring and have the relative attitude angles (roll, pitch, and yaw) within $\pm 10^\circ$ when the Gemini nose enters the docking ring. The Agena docking ring was designed to withstand a maximum longitudinal contact velocity of 1.5 ft/sec (0.46 m/s) and a radial velocity of 0.5 ft/sec (0.15 m/s).

In this simulation the flights were terminated when the value of longitudinal displacement for properly aligned vehicles placed the index bar of the spacecraft in the front plane of the docking ring. The run was considered out-of-tolerance if any one of the docking-ring design limitations was exceeded. Exceeding some of the tolerances does not necessarily mean an actual space mission would be unsuccessful. For example, if one or more of the relative attitude angles or if the transverse displacement of the Gemini nose were out of tolerance, the two vehicles would merely bump together if the relative velocities were low. The pilot could back away and try again, or if these tolerances were only slightly exceeded, some slight additional maneuvering could be used to bring the conditions within tolerance. If the contact velocities are higher than the design values, however, structural damage could occur to the spacecraft, target, or both. The present simulation, which requires all design tolerances to be met and does not permit additional maneuvering after flight termination, should provide more pessimistic results in meeting the docking requirements than those required of an actual space mission.

INITIAL CONDITIONS

The initial conditions used for most of the data presented herein were

x, ft (m)	-250	(-76.20)
y, ft (m)	± 100	(± 30.48)
z, ft (m)	75	(22.86)
ψ , deg		0
θ , deg		0
ϕ , deg		0

All velocities, both linear and angular, were set equal to zero. The paraglider configuration of the Gemini spacecraft with a one-half fuel load was simulated. For the remaining docking flights, longitudinal displacement x was set at -250 feet (-76.20 m), but various transverse displacements, attitude angles, and velocities were employed.

RESULTS AND DISCUSSION

Piloting Techniques

Given complete freedom in the method of effecting a closure from the initial conditions, the pilots (two NASA research pilots and two engineers) utilized two basic approach techniques to align initially the Gemini with the Agena while some distance from the target. One method (fig. 9(a)) involved using the translation jets to null the vertical and lateral displacements while closing longitudinally on the target. At the same time, zero relative angular alignment was maintained. Appropriate initial velocities were selected by the pilot so that the azimuth and elevation angles of the pilot's line of sight to the target would be reduced as range decreased. When the spacecraft's longitudinal axis approached coincidence with the extended longitudinal axis of the target, the opposite vertical and lateral thrusters were fired to stop the transverse motion. If initial conditions imposed angular misalignments of the vehicles, the pilot first oriented his spacecraft to provide zero relative angular alignment. This simply required altering the target's spatial location measured in the Gemini body axis system by spacecraft attitude changes until the target aspect and target location indicated that the spacecraft and target body axes were parallel. This procedure aligned the spacecraft translational thrusters with the target axes.

The second method (fig. 9(b)) consisted of initially rotating the spacecraft and then, by using only the longitudinal thrusters, establishing an intercept course with the extended longitudinal axis of the target. This method supplied the three velocity components relative to the target as in the previous method but required periodic adjustment of the pitch and yaw angles of the spacecraft during the coast phase to compensate for line-of-sight changes and to keep the target in view. By the time the intercept point was reached, the pitch and yaw angles were near the null position and the vertical and lateral translation jets were then used to stop the transverse motion. Roll angle corrections, if needed, were made at this point in the approach.

Either approach could be used by the pilots to establish satisfactory initial relative alignment at distances generally from 50 feet (15.24 m) to 100 feet (30.48 m) from the target. In addition, neither approach provided a decisive performance advantage. In both methods, initial longitudinal velocity \dot{x} of the order of 2 ft/sec (0.61 m/s) was employed. This magnitude was reduced as the intercept point was approached or shortly thereafter to a value considerably below the docking-ring design tolerance. For the resulting coast times encountered, the orbital terms in the equations of motion influence the in-plane vehicle velocities and approach trajectory. These effects however were not

particularly noticed by the pilot who was concerned mainly with achieving initial alinement.

From the position of initial alinement to the flight termination point, the task was one of continually trying to improve the relative alinement. Ideally, the translational and angular misalignments would be reduced as range decreased. For perfect vehicle alinement, relative target location varied with range because of the parallax angle involved. (See fig. 10.) A closure velocity, generally about 1/2 ft/sec (0.15 m/s), was employed during this final portion of the approach. This remained uncorrected up to the termination point unless it was necessary to stop or back away because the pilot became aware of the existence of an out-of-tolerance condition. Thus, by not correcting closing velocity during the final approach, the piloting task is effectively reduced to controlling only 5 degrees of freedom. A more comprehensive treatment of the technique employed and the difficulties involved during the final 50 feet (15.24 m) of separation is presented in reference 7.

Attitude Control Modes

Rate command.- Using the rate-command attitude control mode, the pilot could successfully and consistently perform the docking with a fully illuminated target. The task was not difficult to perform, but a number of practice runs were required to reach a high level of proficiency. After some experience, combined control inputs (particularly in translation) could be used effectively. The tight dead band ($0.1^\circ/\text{sec}$) used in the rate-command attitude control system simplified the pilot's task. One of its major contributions was the elimination of vehicle attitude motions due to control coupling effects when applying vertical and lateral translation inputs. In essence, the tight dead band reduced the docking problem to one of 3 degrees of translation freedom with an occasional correction for attitude alinement. With the attitude controller undeflected, all relative movement between vehicles could be interpreted by the pilot to be primarily translations.

It should be noted that a few data runs (not presented herein) were made with other dead-band settings. At $0.2^\circ/\text{sec}$, the difference in system performance was just noticeable to the pilot. At $0.5^\circ/\text{sec}$, however, some degradation of system performance was noted in that the pilot desiring lower angular drift rates was required to use control inputs of the acceleration command type to maintain spacecraft attitudes. The fact that maximum available rates in the simulation were lower than those of the actual spacecraft was of no significance in docking, since the pilot's control inputs rarely, if ever, approached the maximum value available. For these reasons, dead-band and maximum rate differences between this study and presently accepted Gemini values should have no effect on the docking task and data presented herein.

Direct mode.- Using the direct (acceleration command) attitude control mode, successful docking could be accomplished consistently with a fully illuminated target. The task was difficult for the pilot to learn and numerous flights were required to become proficient. The complexities of an acceleration command system (that of applying a control input to start and to stop a

motion with no damping present) were compounded by the degree of control coupling and control power present.

With the magnitude of control coupling present in Gemini, it was necessary to compensate for the coupling when applying a control input. To illustrate, when applying a vertical or lateral translation input, it was necessary to manipulate not only the translation controller but also the attitude controller in an amount just necessary to compensate for spacecraft pitching or yawing. For the reverse situation when pitch or yaw control inputs are applied, compensating transverse translations were not normally used except for large attitude corrections. The magnitude of the control coupling precluded, in most cases, multiple axis control inputs. The use of small inputs eased the control coupling difficulties. In addition, small inputs were beneficial in handling the control power which was large enough to be troublesome in making corrections when close to the target.

Several visual difficulties became manifest in direct mode docking. Separating overall target motion into six component parts was difficult during the final approach when the relative transverse velocities and angular rates were low. In addition, the presence of a parallax angle complicated the vehicle alignment problem. Reference 6 indicates that pilots (without control tasks) could visually align the vehicles near contact only within 2° to 3° in attitude and 2 to 4 inches (5.08 to 10.16 cm) in nose position. As a result, some displacement (particularly in translation) had to develop before the need of a particular control input could be ascertained with any degree of correctness.

Even with the aforementioned difficulties, pilots could perform successful and proficient docking using the direct control mode. Several pilots (A and E herein), using this simulator and the moving-base simulator of reference 6, became so skillful that it was impossible for an observer to detect from the visual display whether the attitude mode was rate command or direct.

Comparison of Attitude Modes

Pilot ratings.- Pilot evaluations of the Gemini control characteristics were obtained during the investigation in the form of pilot opinion ratings. The Cooper rating schedule that was used is presented in table 1. Research pilots A and B provided ratings for the attitude control characteristics of the spacecraft using both modes of control, and these results are presented in table 2. An examination of the data shows a separation of several rating points between the rate-command and direct modes of attitude control for the paraglider configuration. The rate-command system was rated well in the satisfactory region whereas the direct mode ratings fell just within the unsatisfactory region.

Although this paper is concerned only with the paraglider configuration, one additional spacecraft configuration (parachute) and two additional entries providing ratings (research pilot E and Astronauts) were also included for comparison purposes. These additional data were obtained from a study made subsequent to the present test program. It is interesting to note the improved

TABLE 1.- PILOT OPINION RATING SCHEDULE

Adjective rating	Numerical rating	Description	Mission accomplished
Satisfactory	1	Excellent, includes optimum	Yes
	2	Good, pleasant to fly	Yes
	3	Satisfactory, but with some mildly unpleasant characteristics	Yes
Unsatisfactory	4	Acceptable, but with unpleasant characteristics	Yes
	5	Unacceptable for normal operation	Doubtful
	6	Acceptable for emergency condition only ¹	Doubtful
Unacceptable	7	Unacceptable even for emergency condition ¹	No
	8	Unacceptable - dangerous	No
	9	Unacceptable - uncontrollable	No
Catastrophic	10	Motions possibly violent enough to prevent pilot escape	No

¹Failure of a stability augments.

TABLE 2.- PILOT RATINGS FOR SPACECRAFT CONTROL CHARACTERISTICS

Pilot	Attitude control mode	Pilot rating	
		Paraglider configuration	Parachute configuration
A	Rate command	2	2
	Direct	4	$3\frac{1}{2}$
B	Rate command	2	2
	Direct	$4\frac{3}{4}$	4
E	Rate command	---	$2\frac{1}{2}$
	Direct	---	3
Astronauts average (ref. 9)	Rate command	---	$1\frac{5}{6}$
	Direct	---	$3\frac{1}{4}$

rating given by both pilots A and B for the parachute configuration using the direct mode of control. The main factor for the improvement is the amount of control coupling. For the paraglider configuration, the control coupling was about 35 percent greater than that for the parachute configuration.

It is evident from the identical ratings for both spacecraft configurations that control coupling does not affect the spacecraft handling qualities when the rate-command mode is employed. For the direct mode but with no coupling present (jets firing through the spacecraft center of gravity), pilot ratings less favorable than those for the rate-command mode would be expected. Coupling, depending on its magnitude, provides an additional degradation for the direct mode of control. An extrapolation of the direct attitude mode ratings (table 2) to the uncoupled case would indicate that approximately one-half the difference in ratings between the two modes for the paraglider configuration is due to control coupling and the other half is due to a rate versus acceleration control but with no coupling.

Fuel and time.- Total-fuel and flight-time results for a number of docking flights using both attitude modes of control are presented in figure 11(a), for four subjects. These docking flights were performed using one specific set of initial conditions in order to obtain comparable data. The results are presented in the form of total fuel used as a function of flight time because of the interrelationship of these two performance parameters. Fuel values about 25 pounds (11.34 kg) and above were found to involve stopping the closure rate and backing off to realine the vehicles, because out-of-tolerance conditions existed on the first approach. It should be noted that no restraints on fuel and flight time were specified for the docking flights herein. The data were obtained at various times throughout the test program and consequently some effect of pilot proficiency is involved. The comparisons shown for arbitrary 85-percent and 60-percent data boundaries attempt to segregate the data to account for the preceding three factors. A pilot at peak proficiency using a straight-in approach at essentially a constant closure rate required fuel-consumption and flight-time values within the 60-percent boundary shown. The 85-percent boundary includes flights in which the closure rate was altered but with necessary corrections performed in a reasonably efficient manner. Comparison of the boundaries to assess the effects of attitude control mode indicates a certain area of overlap. In general, it appears that an increase in flight time of 1 to 2 minutes can be expected for task accomplishment when using the direct control mode. The results also indicate that a highly trained pilot using the direct mode would probably use slightly less fuel than when using the rate-command attitude control mode.

The total-fuel results of figure 11(a) have been broken into the fuel used for spacecraft translation (fig. 11(b)) and the fuel used for attitude control (fig. 11(c)). As would be expected, the results show that more fuel is used for spacecraft translation than for attitude control. Also, the comparison of the 60-percent boundaries shows that the fuel saving using the direct mode is divided between the translation and attitude systems.

End conditions.- Values of the relative displacements and velocities, both linear and angular, recorded at the termination points of the various flights are presented in figure 12. The larger number of rate-command data points

presented here as compared with the fuel data of figure 11 is due to the inclusion of docking flights made from different initial conditions. Recorded nose displacements (fig. 12(a)) are very similar for either mode of control; both sets of data show a tendency for the Gemini nose to be displaced vertically upward probably because of the fact that the pilots underestimated the available clearance between the Gemini nose and the docking ring surface. The majority of the data are located within $\pm 1/2$ foot (± 0.15 m) which is one-half of the allowable tolerance. Associated vertical and lateral nose velocities are shown in figure 12(b) and most of the data indicate values of 0.2 ft/sec (0.06 m/s) or less. Longitudinal velocity along the target X-axis (fig. 12(b)) was less than $1/2$ ft/sec (± 0.15 m/s) for 75 percent of the flights and in no case was the $1\frac{1}{2}$ -ft/sec (0.46 m/s) tolerance exceeded. The angular misalignment data of figure 12(c) indicate that roll angles were predominately less than $\pm 5^\circ$. It should be noted that an obvious negative-yaw-angle bias exists in the rate-command data which results from parallax due to the pilot not being located on the spacecraft center line. The negative bias results from the pilot's attempt to align and maintain the index bar near the center of the V-slot in the docking ring during the final few feet of travel. This negative bias is not as evident in the direct mode data; however, in this case control is more difficult and accurate alignment is harder to obtain. Comparison of the angular rate data (fig. 12(d)) for the two modes shows more scatter in the direct-mode data than in the rate-command-mode data. This difference would be expected as a result of the automatic control features of the rate-command mode.

An evaluation of the end conditions (fig. 12) relative to the required docking tolerances to determine successful task achievement is indicated in the following table:

Attitude mode	Percent successful completions	
	4-subject average	Pilot A
Rate command	90	97
Direct	80	95

Pilot proficiency effects are evident in the four-subject average for both control modes, but particularly for the direct-mode dockings. Achievement of a high level of successful completions requires a precision of control during the final few feet of closure (not necessary over entire flight) that requires considerable practice to attain when using the direct control mode. Because of the additional experience in both modes of control, pilot A's percentage of successful completions is considered representative of a highly proficient pilot performing the docking task. It is worth noting as regards actual space-flight tolerances that for the four subjects, only 3 of the 154 rate-command flights and 3 of the 73 direct-mode flights involved out-of-tolerance nose velocities that conceivably might cause some damage to the docking ring.

Effect of Control Power

A brief examination of control power using the direct control mode was made in which the thrusters for both the transverse translation and attitude control systems were decreased in size. Only the spacecraft's longitudinal thrusters remained unaltered. Jet sizes the same as the design value and $1/2$ and $1/4$ of the design value were considered. One set of initial conditions was used for these flights and the initially translating technique of figure 9(a) was employed. The results in the form of pilot opinion ratings, fuel ratios, and flight time ratios are presented in figure 13. All flights were within tolerance at the termination point (100 percent successful) and were made using a fully lighted target vehicle. Visual aids (rear-mounted vertical and horizontal bars) were employed on the target and are described in detail in the section on target lighting. Two flights for each control configuration were performed sequentially by the primary research pilot (pilot A). The different configurations were presented to the pilot in the alphabetical listing shown in the figure. Also presented in figure 13 are a few brief pilot comments on the different configurations.

The design ratio of translation power to attitude control power was considered by the pilot to be good. Pilot A particularly liked the configuration for which the jet sizes for both transverse translation and attitude control were reduced to $1/2$ of the design value for applying corrections at ranges close to the target. At larger ranges, however, he preferred the design values. The order of preference (D, E, B, A, C), as would be expected, coincides with the Cooper ratings given. The off-design points B and E were rated somewhat better than the Gemini design primarily because of the reduced control coupling, even though the pilot felt that the vehicle was not responsive enough in transverse translation. The fuel and flight time ratios are also shown in figure 13 for completeness; however, the ratios are not considered significant.

Effect of Initial Conditions

A number of flights were made (data not included herein) using primarily the rate-command attitude control mode in which the initial Gemini velocities and displacements, both linear and angular, were varied to determine if the pilot could accomplish initial vehicle alinement satisfactorily. Linear velocity components resulting in range rates up to 10 ft/sec (3.05 m/s) angular misalignments up to 30° , and transverse displacements that positioned the target at various locations within the pilot's field of view were employed. Other than the expected influence on fuel consumption and flight time, the effect of these initial conditions on establishing initial vehicle alinement was inconsequential. Initially the pilots evaluated the situation presented, applied controls to eliminate the undesirable features, and proceeded to establish a desired approach depending on initial linear displacements. From this point on the piloting technique was essentially the same regardless of the initial conditions and is the reason why most of the data presented herein were obtained from one given set of initial conditions.

Effect of Target Lighting

Mission analyses have shown that for certain Gemini and Agena launch and rendezvous firing schedules, darkside docking is a definite possibility. For such an event, initial considerations for lighting the target specified illumination of only the inner surface of the Agena docking ring. In order to examine the proposed lighting scheme and to explore briefly the darkside problem area in general, a series of docking flights were made using the rate-command attitude control mode. The essential results of these tests are shown in figure 14. Data for a fully illuminated target are presented for comparison. The results show a degradation in performance in that both fuel consumption and flight time increased for darkside operations. More importantly, however, the percentage of successful completions decreased as compared with those for a fully illuminated target. The basic problem encountered here was simply a loss in the visual alinement cues providing boresight. Also presented in the figure are results showing that the use of visual aids on the Agena target vehicle can supply the necessary visual cues to raise the docking performance at night to about the level of daytime docking. The visual aids (three and four light arrangements) that were employed are shown in figure 15 and were the most successful of several that were tried. The addition of the fourth light on the one visual-aid configuration provided better information on roll alinement and, in addition, a better reference for proper location for the index light near contact. The arrangements considered the mechanization problem and were envisioned as spring-loaded flip-out posts. For all dark-side dockings using visual aids, the index bar on the Gemini nose was also illuminated. It should be noted that the proximity of the flashing acquisition light near the line-of-sight light was annoying and for full-scale intensity might cause visual difficulty. However, relocating the three acquisition lights or switching them off during final approach would eliminate this undesirable feature. More information on Gemini-Agena darkside docking, which is in agreement with the results presented herein is available in references 6 and 7.

In addition to darkside dockings and those with a fully illuminated target, a number of flights were made for a partially sun-lit configuration. The lighting configuration used and the primary results of interest are shown in figure 16. With the sun's rays illuminating only the upper half of the Agena, some loss of visual information occurs in the upper area of the docking ring. The piloted flights, however, indicate that no degradation was obtained in the accomplishment of successful docking. This was due to the fact that pilots C and D utilized the illuminated upper surface of the Agena for alinement and pilots A and B used, in addition, the solid white bar aids depicted in the figure. Partial illumination would appear to cause difficulty similar to darkside docking only for target illuminations in which the V-slot and upper side of the target were either entirely or partially unlit. For such cases, visual aids would be helpful.

Effect of Target Yaw Oscillation

For the preceding portions of this investigation, the Agena target was assumed to be rigidly stabilized such that the Z_t -axis always pointed toward

the center of the earth and the X_t -axis remained in the orbital plane. Practical considerations, however, indicate that automatic stabilization systems will always permit some target motion. In order to examine briefly target motion effects, a series of docking flights were undertaken in which the target was oscillated in a single degree of freedom about its center of gravity which was assumed to be on the target X-axis at the target midlength point. Target yaw angle was chosen as the variable and was driven sinusoidally for convenience. Docking flights were made for oscillation amplitudes of $\pm 1^\circ$, $\pm 2.5^\circ$, and $\pm 5^\circ$ and oscillation periods of 10, 20, 40, and 60 seconds to determine those combinations at which difficulty would be encountered in successful task accomplishment. A fully illuminated target vehicle with no visual aid present was employed. The results of these tests are presented in figure 17 to 22.

Figure 17 shows the successfulness of task accomplishment as a function of target oscillation amplitude and period. The data shown are the combined results for four subjects (pilots A and B, engineers C and D) using both the rate-command and direct attitude control modes. A total of 97 data flights was made. For 25 percent of these, direct mode control was used and most of these direct flights were made by the primary research pilot, pilot A. To account for subject differences, the results are presented in nondimensional ratio form. The data of figure 17(a) showing the effect of oscillation amplitude indicate that at amplitudes of $\pm 2.5^\circ$ or less, no difficulty in docking was encountered. Difficulty, however, occurred at an oscillation amplitude of $\pm 5^\circ$ (fig. 17(a)) and was a function of oscillation period (fig. 17(b)) where the number of successful docking flights decreased with decreasing period. The trend of the data with period was typical for each of the four subjects.

Pilot ratings (fig. 18) at the various oscillation periods for a constant amplitude motion of $\pm 5^\circ$ were supplied by pilot A for docking flights using both the rate-command and direct attitude control modes. As would be expected, the ratings become less desirable as period is decreased. With the rate-command attitude control mode, pilot A was more successful in completing the dockings within the required tolerances for the two shorter oscillation periods tested than were the other three subjects, and consequently his ratings at these periods would be more favorable than would those of the other subjects. Several of the docking flights at the shorter periods were made for which target oscillation proved to be no problem whatsoever. For these flights target motion supplied the corrections necessary for successful docking. All four subjects experienced this occurrence at least once. For rating purposes, such a flight was rescheduled.

Of the various terminal conditions available from the docking flights with an oscillating target, the position of the target in its cycle at the flight termination point is of particular interest in view of the sinusoidal target motion employed. Figure 19 presents the target yaw-angle results obtained. The distribution curve for all of the data flights performed is given in figure 19(a). This curve is compared in figure 19(b) with a calculated curve obtained from consideration of only the target sinusoidal motion. The calculated curve is based on the relative time the target spends at different positions throughout a quarter cycle of the oscillation and, consequently, is the distribution curve that would be expected if angular position of the target in

its cycle was of no significance to the pilot during the docking task. The distribution curve for $\pm 1^\circ$ and $\pm 2.5^\circ$ amplitude data (if sufficient flights were available) should closely duplicate the calculated curve since the presence of an oscillation is inconsequential to task accomplishment, because the movement of the target nose is small and well within the docking tolerance for lateral displacement. The apparent outward shift of the measured data in the maximum-amplitude region is undoubtedly due to the fact that most of the data were obtained at $\pm 5^\circ$ amplitude. For $\psi_{t,max}$ of $\pm 5^\circ$, the lateral movement of the target nose for the center-of-gravity position assumed herein is very nearly the docking tolerance, and changes in target aspect due to the oscillatory motion are readily discernible. Figure 19(c) illustrates for the $\pm 5^\circ$ amplitude data that as oscillation period decreases, target yaw angle at flight termination tends to approach maximum amplitude. Although the data of figure 19(c) would appear to indicate the judicious choice by the pilot of maximum target yaw angle for nose insertion at the shorter periods, such was not the case. In fact, it was almost impossible to tell with any degree of certainty what point of the target cycle was being observed. The difficulty resulted simply because the relative motion of the target consisted not only of the target's yawing motion but the Gemini's translations and rotations as well. In actuality, most of these flights required the pilot to stop the closure rate just a few feet from contact and to apply alinement corrections. Once the alinement appeared within tolerance, the closure was completed. Since changes in target yaw angle were small for a short period of time near maximum amplitude, the pilot was afforded an opportunity to accomplish the corrections required without realizing the position of the target in its cycle.

Some typical fuel and flight time results from the oscillation tests are presented in figure 20 showing the effect of oscillation period and amplitude. The data presented at a given amplitude were obtained as a single group of tests, and consecutive flights were made at decreasing values of oscillation period. The results, in general, indicate an increase in fuel and flight time with decreasing period for the $\pm 5^\circ$ amplitude data. The lower values shown for the 10-second-period data for pilot D are typical of the fortuitious circumstances described previously. Most of the tests, however, were not made in the consistent manner of decreasing period for consecutive flights; consequently, some scatter of the data was obtained. All the $\pm 5^\circ$ -amplitude test data are presented in figure 21 in ratio form to account for the individual characteristics of the subjects in performing the docking task. The results are similar to those in figure 20 in that average fuel and flight time increased with decreasing period. It should be noted that the increases shown for total fuel in figures 20 and 21 result from an increase in both the translation and attitude fuel. In addition, figure 22 presents a comparison of the rate-command and direct data obtained from docking flights made by pilot A. The addition of target oscillatory motion at $\pm 5^\circ$ amplitude increased the task difficulty to the extent that pilot A required more fuel and flight time for task accomplishment with the direct mode than with the rate-command mode.

Effect of Star Background

The docking flights performed herein were made both with and without the use of a star background. The presence of the star field was found to be of little value even for the tests involving the oscillating target. In fact, the only time the star field was utilized was when maneuvers were performed which resulted in the target vehicle disappearing from the field of view of the pilot's window, such as during the initial thrusting period when the spacecraft was aimed so as to intercept the target's longitudinal axis (fig. 9(b)). With the star field present, the pilot could aim for an intercept point somewhat further removed from the target than he could without the star field. During the final approach, the pilot was concentrating so exclusively on the target that he ignored the star field completely.

CONCLUSIONS

A full-size Gemini-Agena docking study was made using a visual docking simulator to determine the effects of spacecraft attitude-control mode, control power, target lighting, and one-degree-of-freedom target oscillatory motion. Flights were initiated at a range of about 300 feet (91.44 m) and were performed using both the rate-command and direct attitude control modes. Only visual cues obtained from observation of the target through the spacecraft window were used for guidance information. Vehicle mass and moments of inertia simulated the paraglider configuration of the Gemini spacecraft with one-half fuel load. The results of the study apply to a stabilized and fully illuminated target vehicle unless specified otherwise and are as follows:

1. The rate-command attitude control system was found to be well suited for the docking task. Consistent and successful docking could also be obtained with the direct control mode (acceleration command), but the task was difficult to learn and required considerable practice to become proficient.
2. Primary pilot ratings (Cooper scale) on the Gemini attitude handling characteristics were 2 when using the rate-command attitude control mode and 4 when using the direct mode.
3. Comparison of the fuel and flight-time results for the two attitude control modes indicated that when using the direct mode, flight times 1 to 2 minutes longer were needed than with the rate-command mode; however, slightly less fuel would be required by a proficient pilot using the direct mode.
4. End conditions for docking flights using both modes of attitude control show
 - a. Longitudinal velocities were $1/2$ ft/sec (0.15 m/s) or less for 75 percent of the flights. Design tolerance of 1.5 ft/sec (0.46 m/s) was never exceeded.

b. Most vertical and lateral relative nose velocities were within ± 0.2 ft/sec (± 0.06 m/s).

c. Majority of data for vertical and lateral nose displacements were within $\pm 1/2$ foot (± 0.15 m/s).

d. Roll angles were predominately less than $\pm 5^\circ$.

e. Pitch and yaw angles were scattered randomly with most of the data within the design tolerance of $\pm 10^\circ$.

5. Results obtained by one research pilot on the effect of control power (obtained by decreasing thruster size only) for direct mode control indicate that the design ratio of attitude to translation control power was good. Jet sizes one-half those of the present design were preferred for maneuvering the Gemini when close to the target; however, the design thrust levels were desired for operations some distance away.

6. For darkside docking using the rate-command control mode, performance degradations occurred when only the docking ring was illuminated because of a lack of boresight information. With the addition of visual aids to supply this information, darkside docking results comparable to daytime results were obtained. Docking flights with a partially illuminated Agena in which the V-slot and upper portions of the target were illuminated could be accomplished with daytime success.

7. Using both attitude control modes, results of single-degree-of-freedom oscillation in yaw tests with a fully illuminated target indicated a negligible influence of target motion on docking success for motion amplitudes of $\pm 1^\circ$ and $\pm 2.5^\circ$ and oscillation periods from 60 to 10 seconds. For $\pm 5^\circ$ amplitude motion, however, successful completions decreased with attendant increases in fuel consumption and flight time as a function of decreasing oscillation period for periods less than 60 seconds.

Langley Research Center,
National Aeronautics and Space Administration,
Langley Station, Hampton, Va., July 21, 1965.

APPENDIX A

EQUATIONS USED IN SIMULATION

A schematic diagram of the equations as programmed is presented in figure 23. Vehicle mass, moments of inertia, and center-of-gravity location were held constant during the investigation, since total-fuel consumption provided only negligibly small changes in these parameters for most of the docking flights.

FORCE EQUATIONS

The force equations are written with respect to a rotating set of reference axes located in the orbiting Agena. (See fig. 1.) The rotating axes are oriented such that the Z-axis is always directed along the local vertical and pointing toward the center of the earth. The X-axis is constrained to lie in the orbital plane. The Agena body axes and the reference axes are assumed coincident at all times when the target is not oscillating and maintained so by the Agena's stabilization system. Using a first-order approximation to the gravity field, the equations are as follows:

$$\frac{F_X}{m} = \ddot{x} + 2\omega\dot{z}$$

$$\frac{F_Y}{m} = \ddot{y} + \omega^2 y$$

$$\frac{F_Z}{m} = \ddot{z} - 2\omega\dot{x} - 3\omega^2 z$$

Terms including ω^2 were found to be too small to be significant for problem scaling on the computer and thus were neglected. Similar equations have been used previously in a number of rendezvous studies. (For example, see refs. 10 and 11.)

MOMENT EQUATIONS

The moment equations were written with respect to a body system of axes with the origin located at the center of gravity of the Gemini spacecraft. The center of gravity was chosen to correspond to a one-half-fuel-load condition for the paraglider configuration. The moment equations used are

APPENDIX A

$$M_{X,b} = \dot{p}I_{X,b} + qr(I_{Z,b} - I_{Y,b}) + (r^2 - q^2)I_{YZ,b} + (pr - \dot{q})I_{XY,b} - (pq + \dot{r})I_{XZ,b}$$

$$M_{Y,b} = \dot{q}I_{Y,b} + pr(I_{X,b} - I_{Z,b}) + (pq - \dot{r})I_{YZ,b} - (qr + \dot{p})I_{XY,b} + (p^2 - r^2)I_{XZ,b}$$

$$M_{Z,b} = \dot{r}I_{Z,b} + pq(I_{Y,b} - I_{X,b}) + (q^2 - p^2)I_{XY,b} - (pr + \dot{q})I_{YZ,b} + (qr - \dot{p})I_{XZ,b}$$

FORCE TRANSFORMATION

In order to solve the three translational equations of motion, the forces F_X , F_Y , and F_Z acting on the Gemini spacecraft in the direction of the rotating axes are required. These were obtained using the forces generated along the Gemini spacecraft body axes by the various thrusters together with a conventional Euler-angle matrix. The following matrix was employed:

$$\begin{Bmatrix} F_X \\ F_Y \\ F_Z \end{Bmatrix} = \begin{Bmatrix} a_1 & a_2 & a_3 \\ b_1 & b_2 & b_3 \\ c_1 & c_2 & c_3 \end{Bmatrix} \begin{Bmatrix} F_{X,b} \\ F_{Y,b} \\ F_{Z,b} \end{Bmatrix}$$

where, for order of rotation ψ , θ , and ϕ

$$a_1 = \cos \theta \cos \psi$$

$$a_2 = \cos \psi \sin \theta \sin \phi - \sin \psi \cos \phi$$

$$a_3 = \cos \psi \sin \theta \cos \phi + \sin \psi \sin \phi$$

$$b_1 = \sin \psi \cos \theta$$

$$b_2 = \sin \psi \sin \theta \sin \phi + \cos \psi \cos \phi$$

$$b_3 = \sin \psi \sin \theta \cos \phi - \cos \psi \sin \phi$$

$$c_1 = -\sin \theta$$

$$c_2 = \cos \theta \sin \phi$$

$$c_3 = \cos \theta \cos \phi$$

APPENDIX A

EULER RATE EQUATIONS

The rate of change of the Euler angles measured between the rotating reference axes and the Gemini body axes is given by the following equations:

$$\dot{\psi} = \frac{r \cos \phi}{\cos \theta} + \frac{q \sin \phi}{\cos \theta} - \omega \tan \theta \sin \psi$$

$$\dot{\theta} = q \cos \phi - r \sin \phi - \omega \cos \psi$$

$$\dot{\phi} = p + q \tan \theta \sin \phi + r \tan \theta \cos \phi - \frac{\omega \sin \psi}{\cos \theta}$$

where $\omega = 0.0012$ radian per second and is the angular velocity of the Agena in a 150-nautical-mile (277.8-km) circular orbit.

FUEL CONSUMPTION

The amounts of fuel used for control along and about each axis of the Gemini spacecraft were measured independently. Values for translation, attitude, and total fuel were obtained by summing the appropriate components. The general expression as applied to each component is

$$\text{Pounds of fuel} = \sum_{\eta=0}^{\eta=N} \frac{(\text{Jet thrust in lb})}{I_{sp}} \Delta t_n$$

where $\eta = N$ is the total number of inputs of a particular control made during a docking flight and Δt_n is the time of each given control input.

TARGET OSCILLATION

The computer portion of the gunnery trainer as constructed included the capability of performing an axis transformation associated with a conventional set of target Euler angles. This additional capability permitted the target body axes not only to be misaligned but also manipulated with respect to the reference axes. For the docking flights performed herein, the target Euler angles (yaw, pitch, and roll) were set and maintained at zero except for the oscillation tests at which time the target yaw angle was driven according to the following equation:

$$\psi_t = \psi_{t,\max} \sin \frac{2\pi}{P} t$$

REFERENCES

1. Fox, J. C.; and Windeknecht, T. G.: Six Degree-of-Freedom Simulation of Manned Orbital Docking System. 9352.8-37, Space Tech. Labs., Inc., Apr. 1962.
2. Montgomery, James E.: Manned Control of Space Vehicle Docking. Vol. 16, pt. one of Advances in the Astronautical Sciences, Norman V. Petersen, ed., Western Periodicals Co. (N. Hollywood, Calif.), c.1963, pp. 147-161.
3. Little, Alfred C.: A Manned Docking Simulator With Five Degrees of Freedom. Vol. 16, pt. one of Advances in the Astronautical Sciences, Norman V. Petersen, ed., Western Periodicals Co. (N. Hollywood, Calif.), c.1963, pp. 497-506.
4. Riley, Donald R.; and Suit, William T.: A Fixed-Base Visual-Simulator Study of Pilot Control of Orbital Docking of Attitude-Stabilized Vehicles. NASA TN D-2036, 1964.
5. Langley Research Center Staff: A Compilation of Recent Research Related to the Apollo Mission. NASA TM X-890, 1963.
6. Pennington, Jack E.; Hatch, Howard G., Jr.; Long, Edward R.; and Cobb, Jere B.: Visual Aspects of a Full-Size Pilot-Controlled Simulation of the Gemini-Agena Docking. NASA TN D-2632, 1965.
7. Hatch, Howard G., Jr.; Riley, Donald R.; and Cobb, Jere B.: Simulating Gemini-Agena Docking. Astronaut. Aeron., vol. 2, no. 11, Nov. 1964, pp. 74-81. (Also available as NASA RP-417.)
8. Mechtly, E. A.: The International System of Units - Physical Constants and Conversion Factors. NASA SP-7012, 1964.
9. Jaquet, Byron M.; and Riley, Donald R.: An Evaluation of Gemini Hand Controllers and Instruments for Docking. NASA TM X-1066, 1965.
10. Eggleston, John M.: A Study of the Optimum Velocity Change to Intercept and Rendezvous. NASA TN D-1029, 1962.
11. Eggleston, John M.; and Beck, Harold D.: A Study of the Positions and Velocities of a Space Station and a Ferry Vehicle During Rendezvous and Return. NASA TR R-87, 1961.

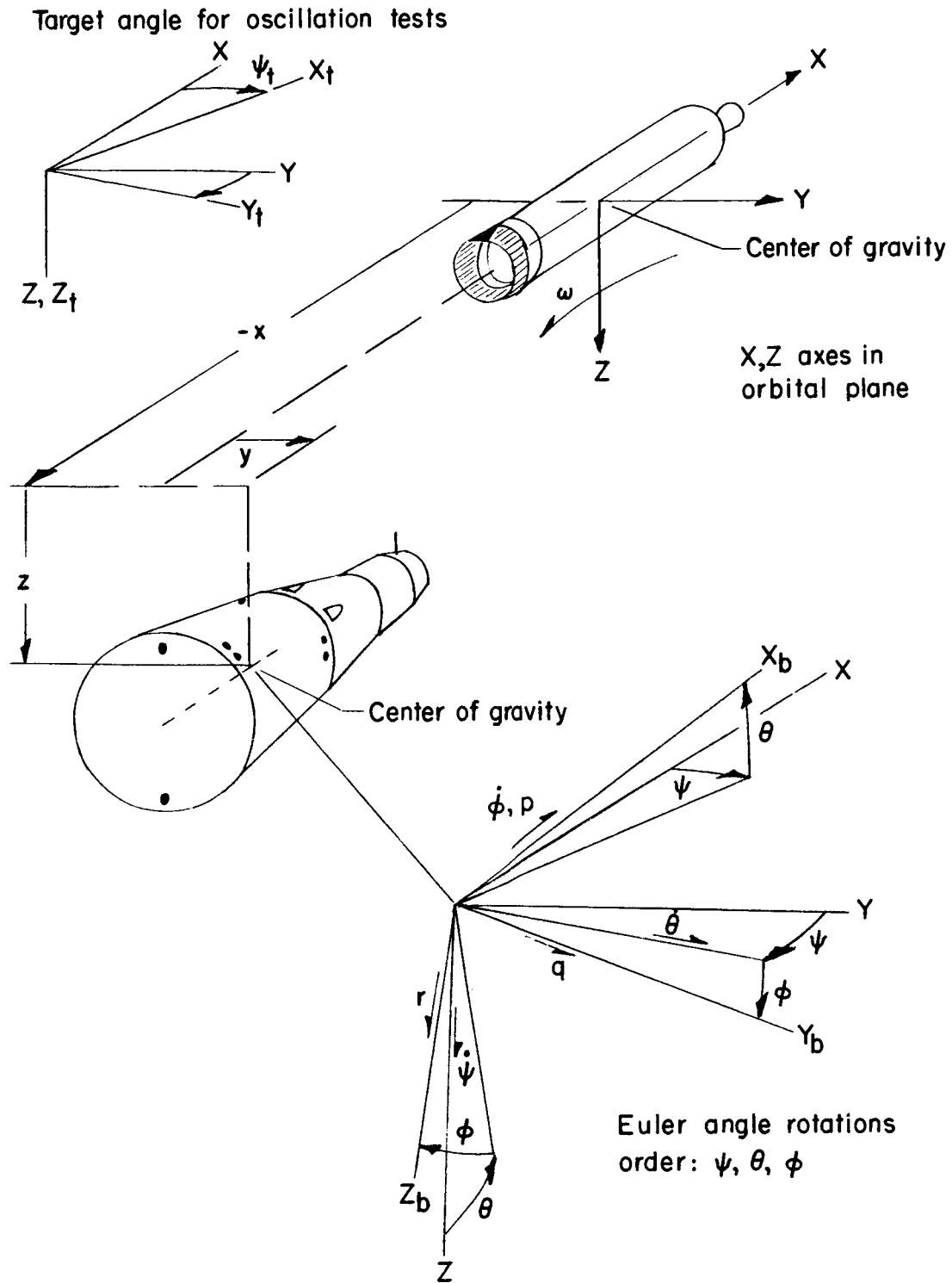
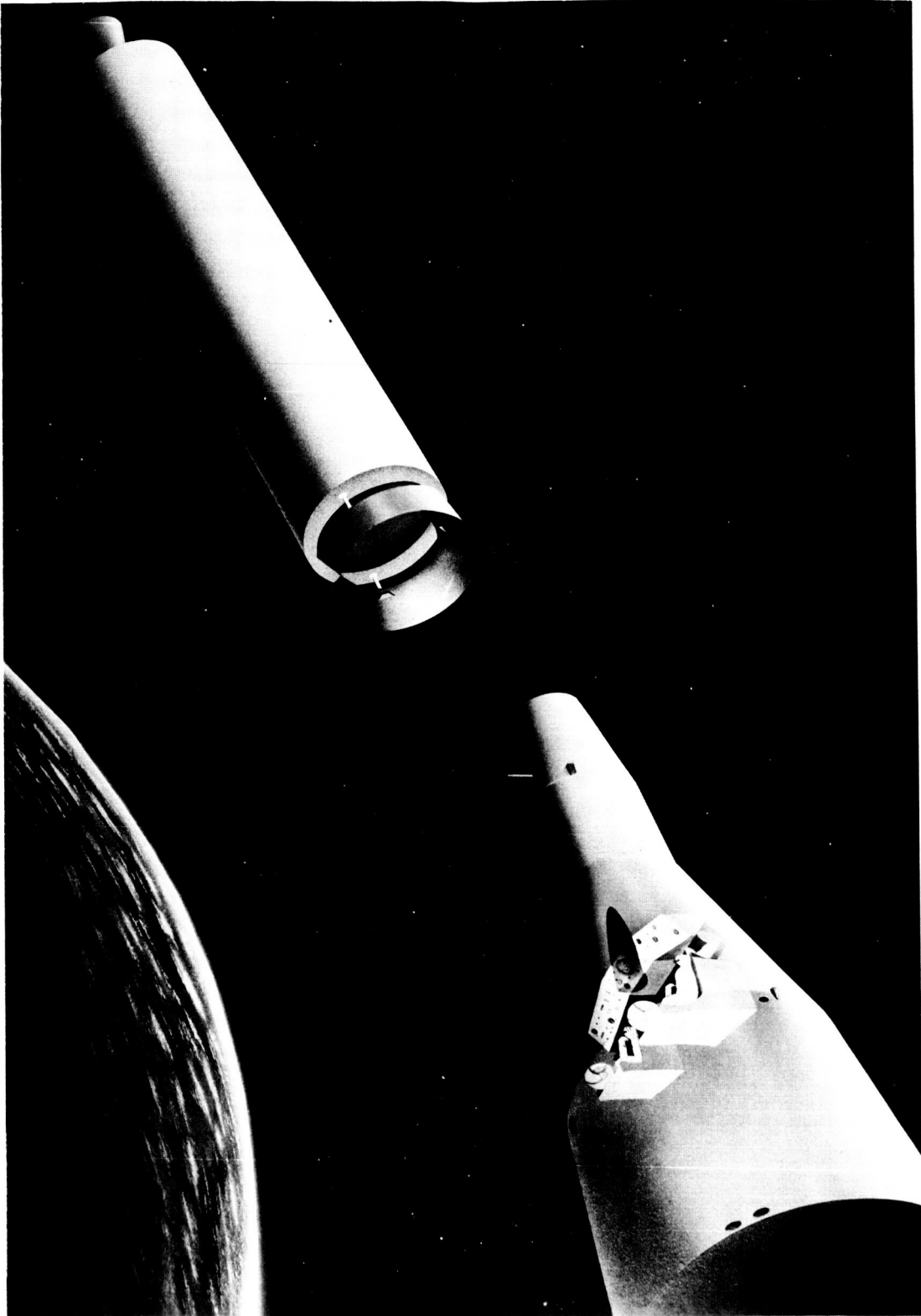
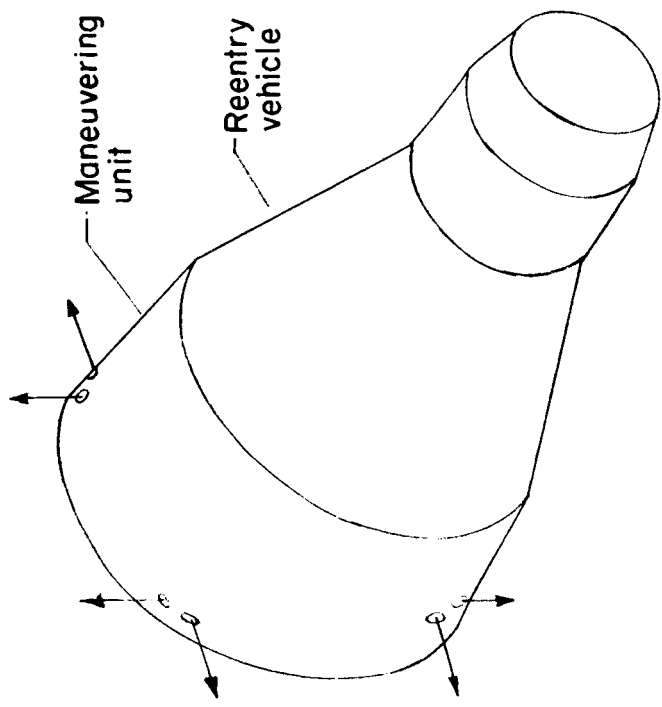


Figure 1.- System of axes used.

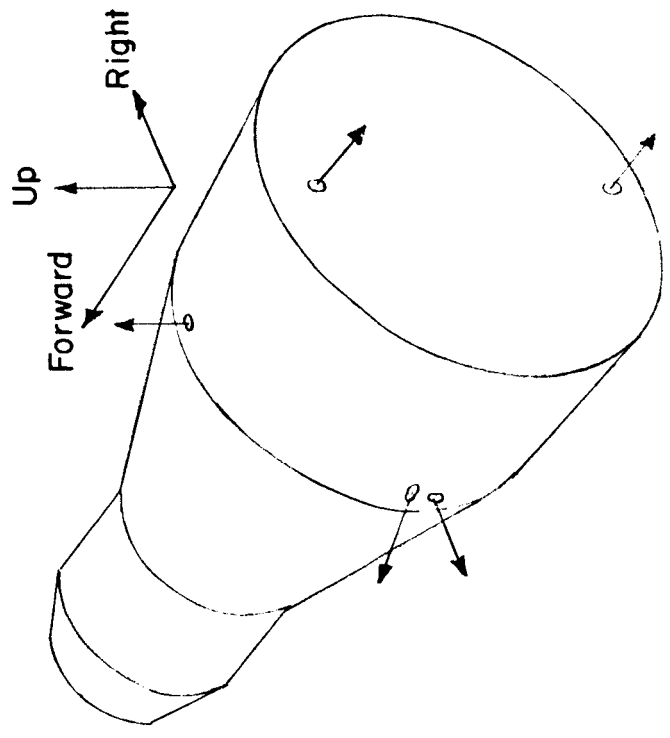


L-62-3375

Figure 2.- Artist's illustration of Gemini and Agena vehicles during the docking maneuver.



Attitude control



Translation control

Figure 3.- Gemini spacecraft orbital attitude and maneuvering system.

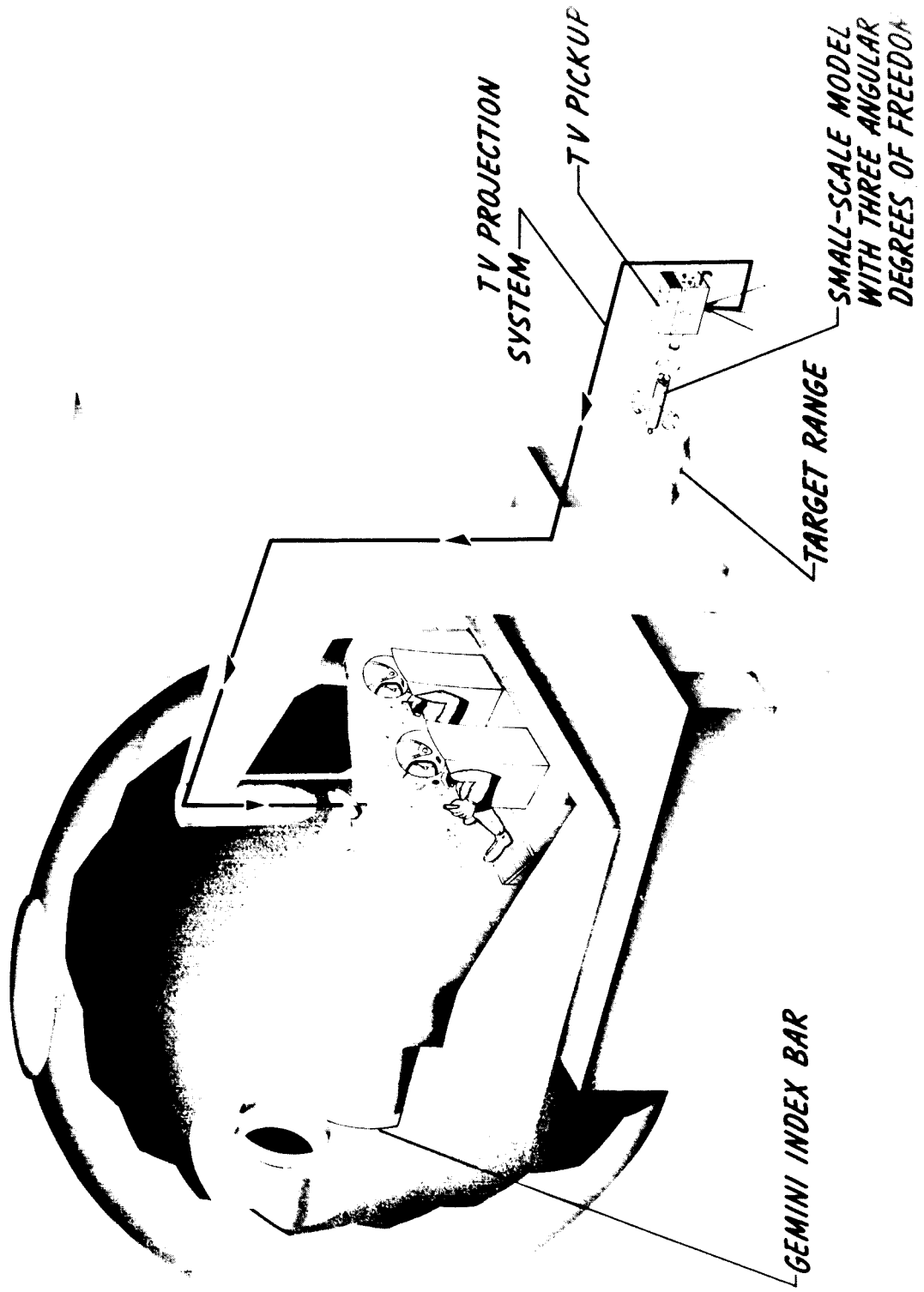


Figure 4.- Artist's isometric sketch of fixed-base visual docking simulator.

L-62-3376

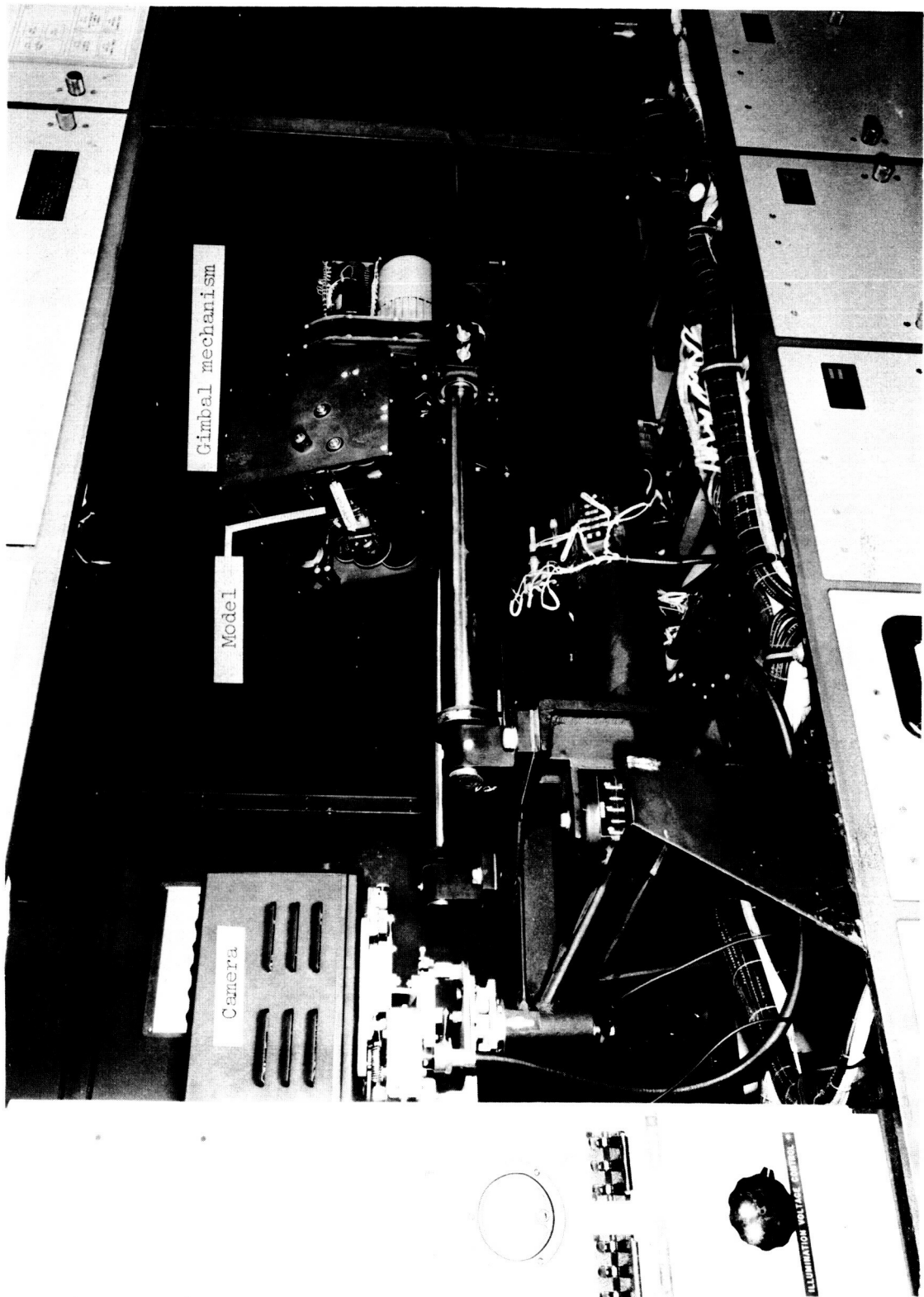


Figure 5.- Television pickup camera, Agena model in gimbal box, and range bed.

L-62-172.1

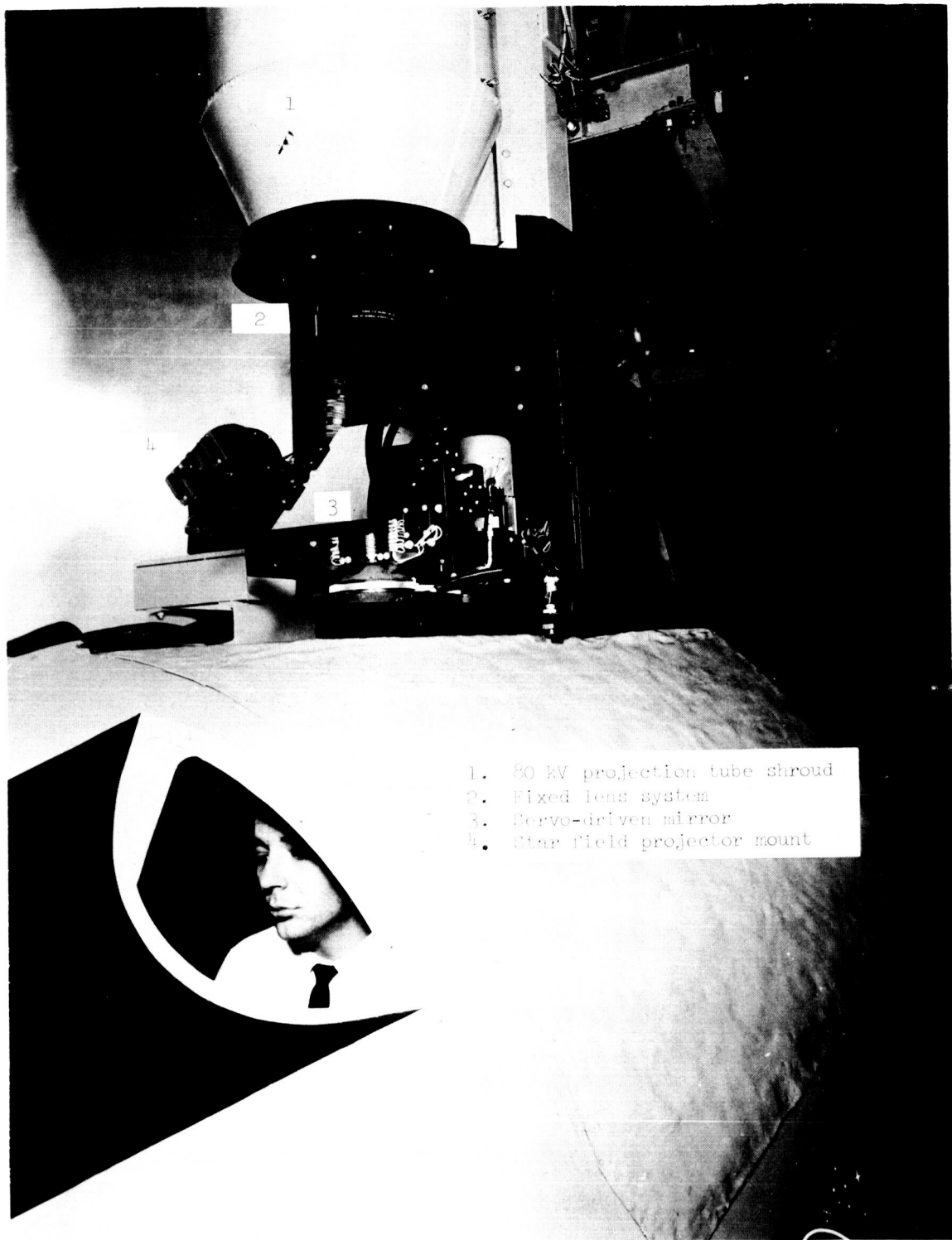
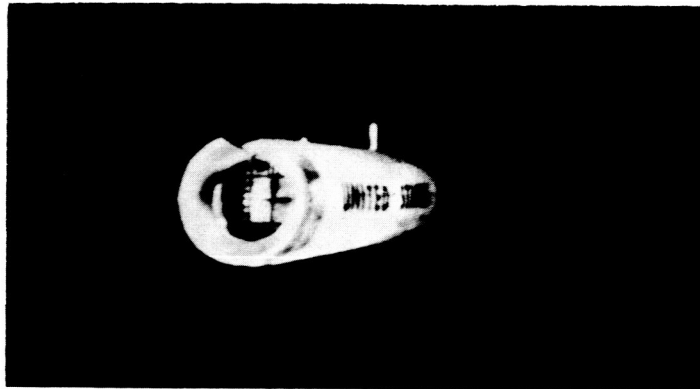
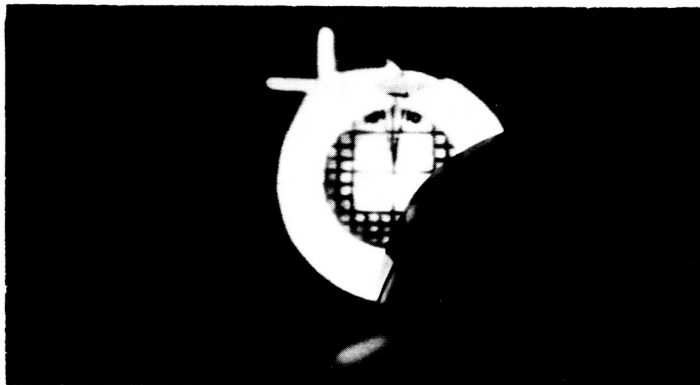


Figure 6.- External view of Gemini mock-up with television projection system.

L-62-167.1



(a) Gemini displaced to right of target.



(b) Gemini and Agena center lines aligned a short distance from contact.



(c) Gemini located above target.

L-65-167

Figure 7.- Photographs of target image displayed on spherical screen showing target markings employed in simulation. (Large squares in center photo represent ± 1 -foot (0.30-m) docking tolerance. Vertical and horizontal bars are visual aids used.)

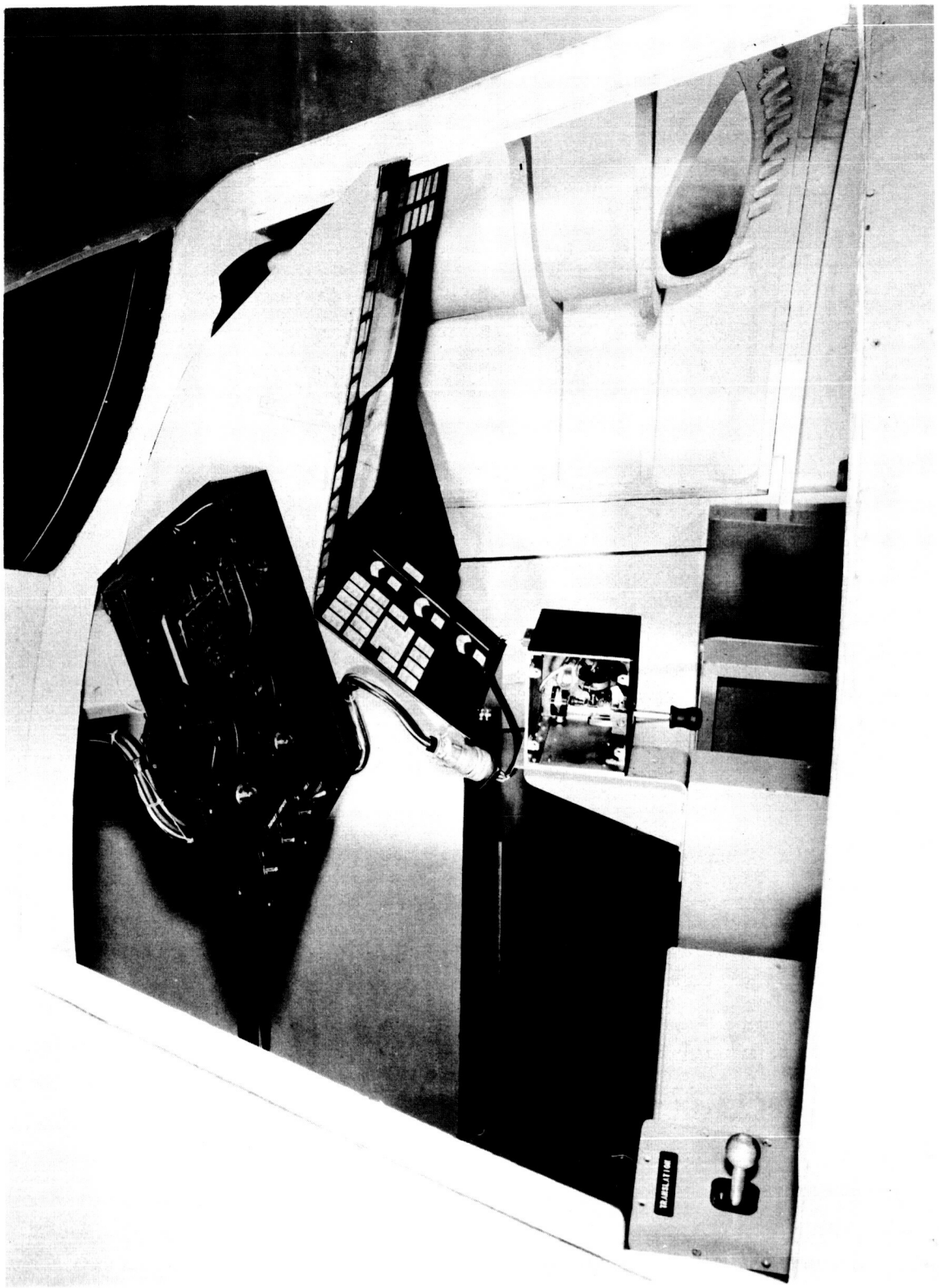
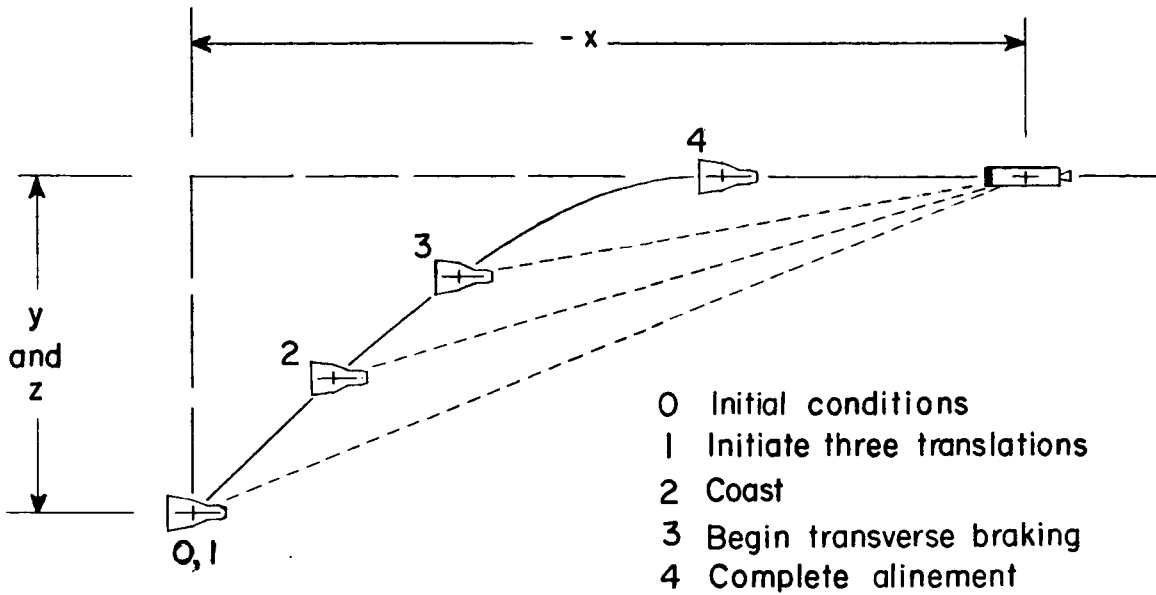
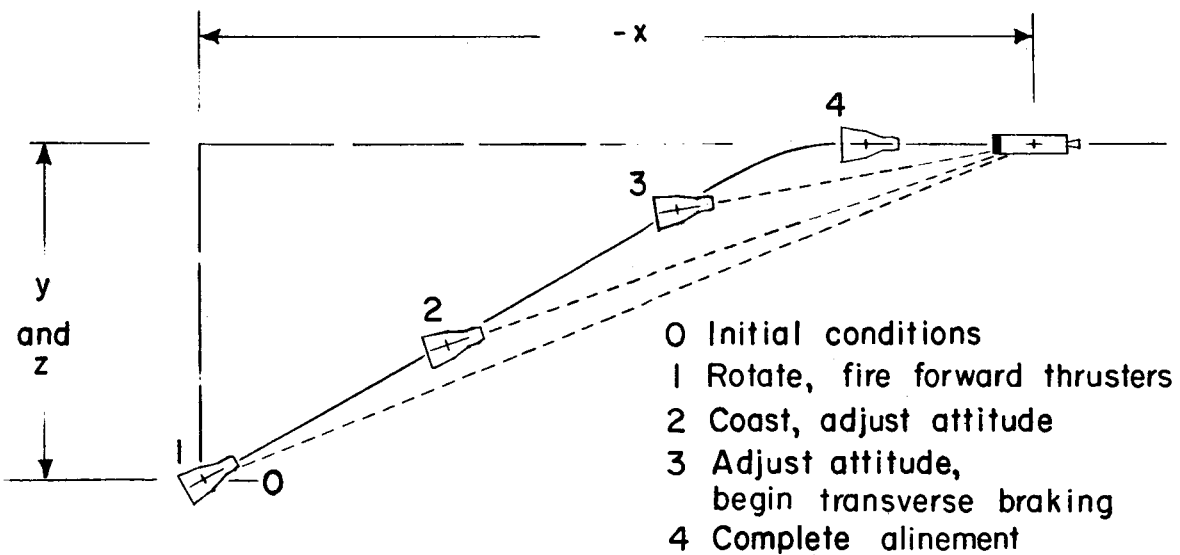


Figure 8.- Photograph of Gemini mock-up with the window panel removed showing the instrument panel and finger-tip controllers employed. L-62-171



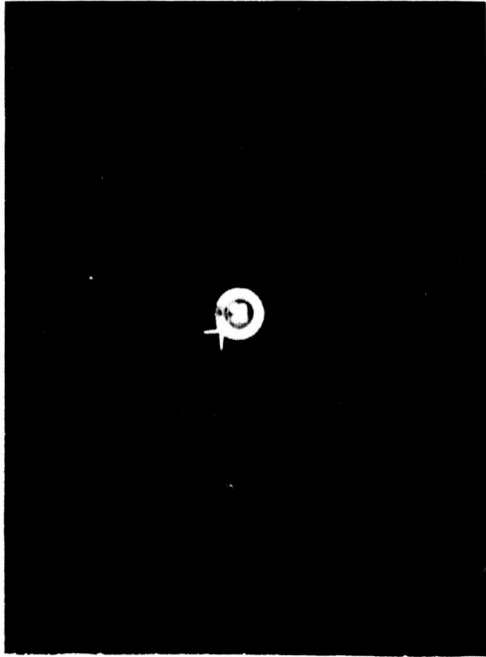
(a) Translating while maintaining zero relative attitude alinement with target.

—————Spacecraft trajectory
 - - - - -Line of sight

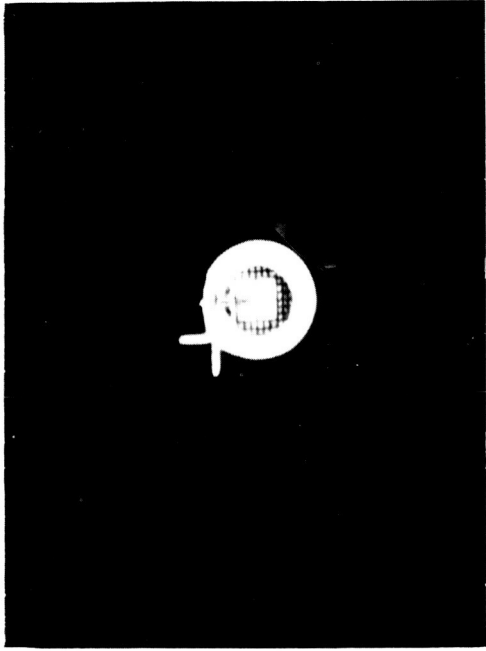


(b) Reorient spacecraft attitude and establish intercept course.

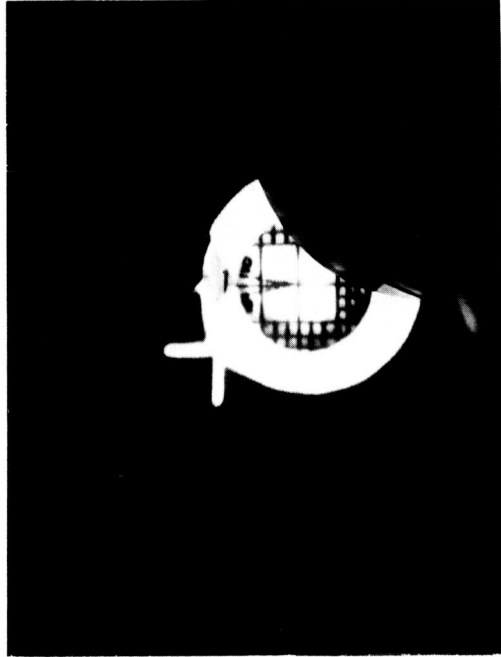
Figure 9.- Illustration of two techniques employed for establishing a closure course on target.



(a) Line-of-sight range about 80 feet (24.38 m).



(b) Line-of-sight range about 37 feet (11.28 m).

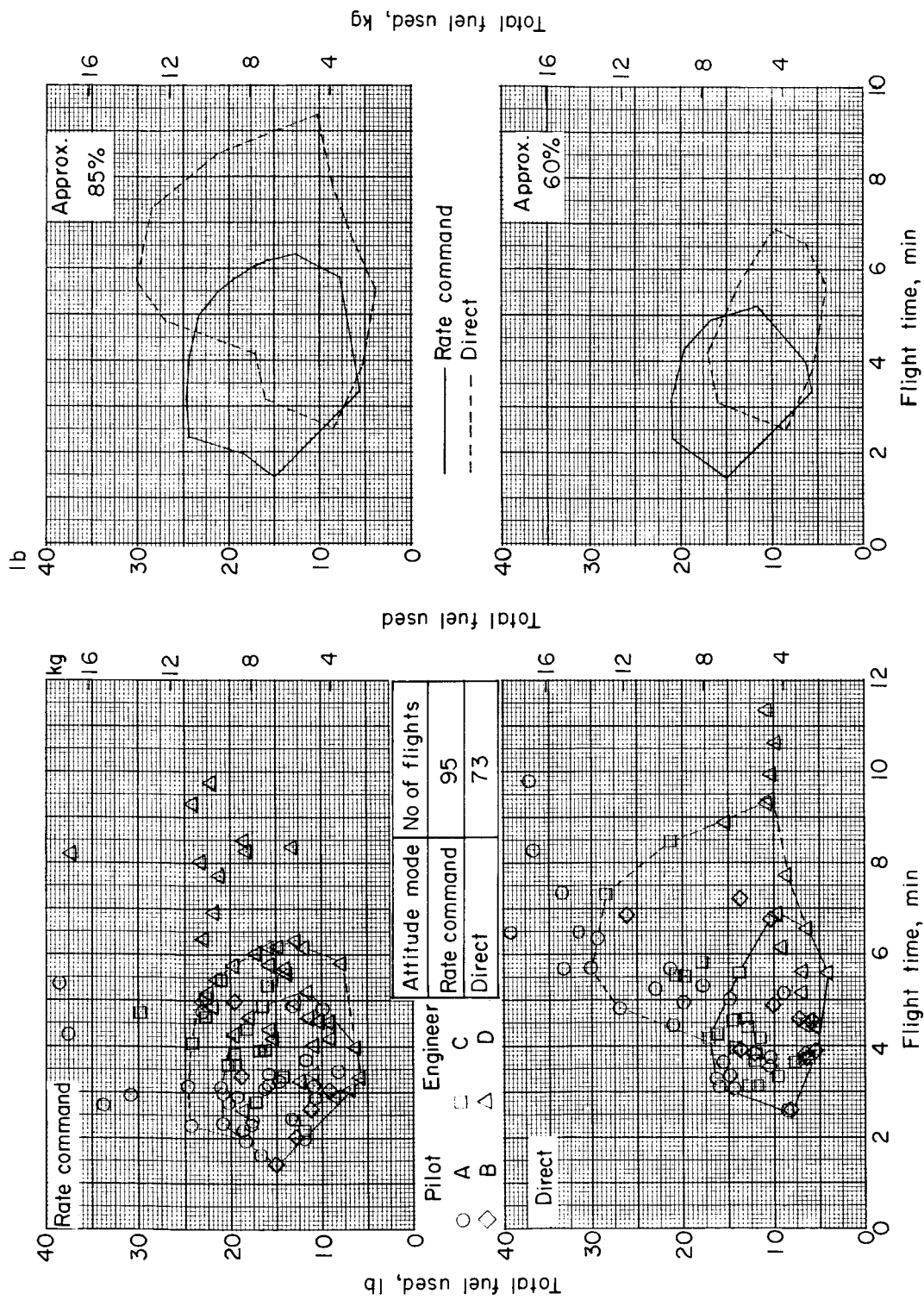


(c) Line-of-sight range about 20 feet (6.1 m).



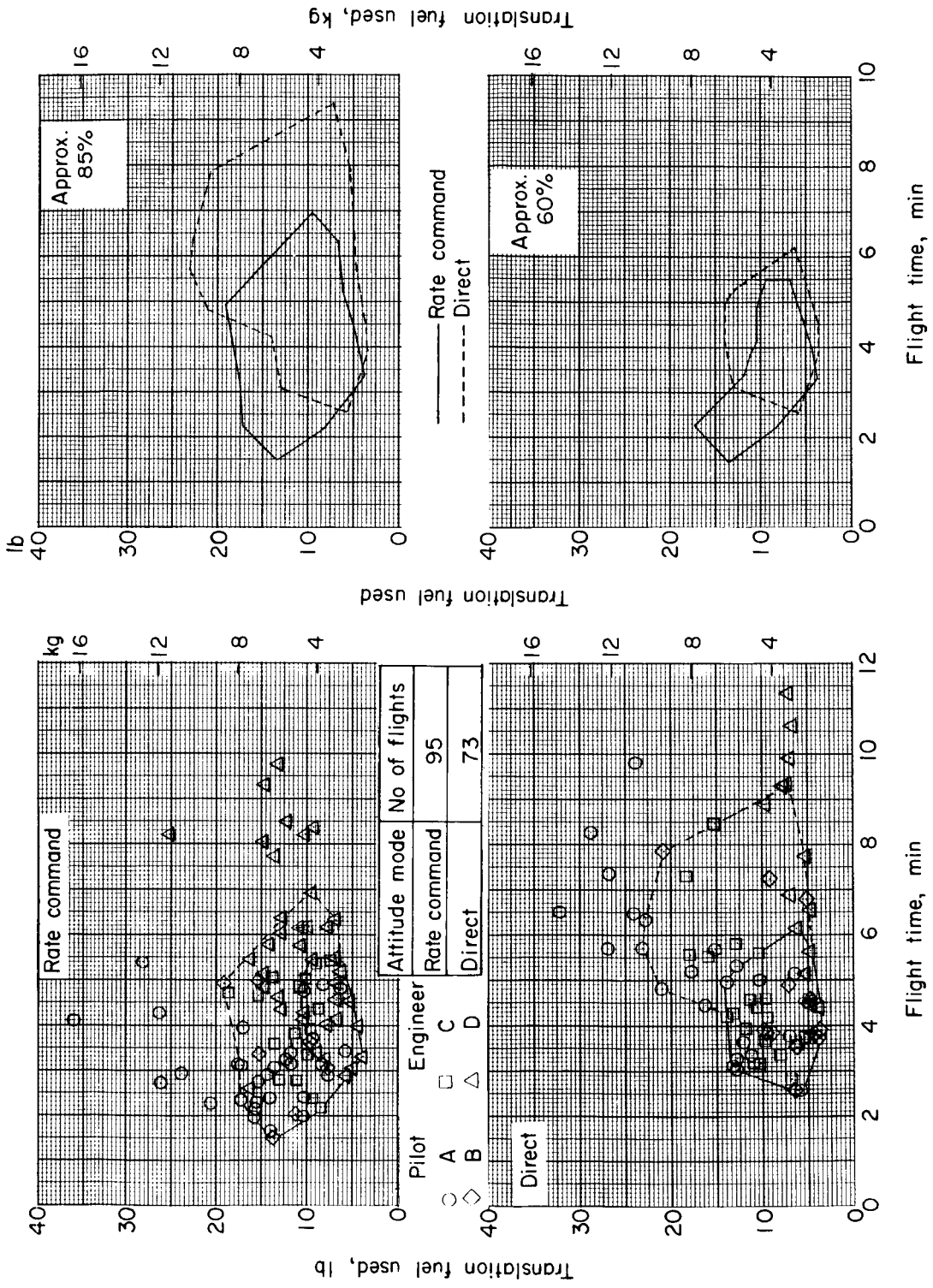
(d) Line-of-sight range about 10 feet (3.05 m) (terminal docking position). L-65-168

Figure 10.- Photographs of target image taken with camera located at the position of the pilot's eyes showing the effect of parallax angle with various values of line-of-sight range. Gemini and Agena center lines aligned. Relative attitude angles are zero. (Note: for perfect vehicle alignment shown, pilot's line of sight parallel to Gemini center line passes through intersection of two visual-aid bars.)



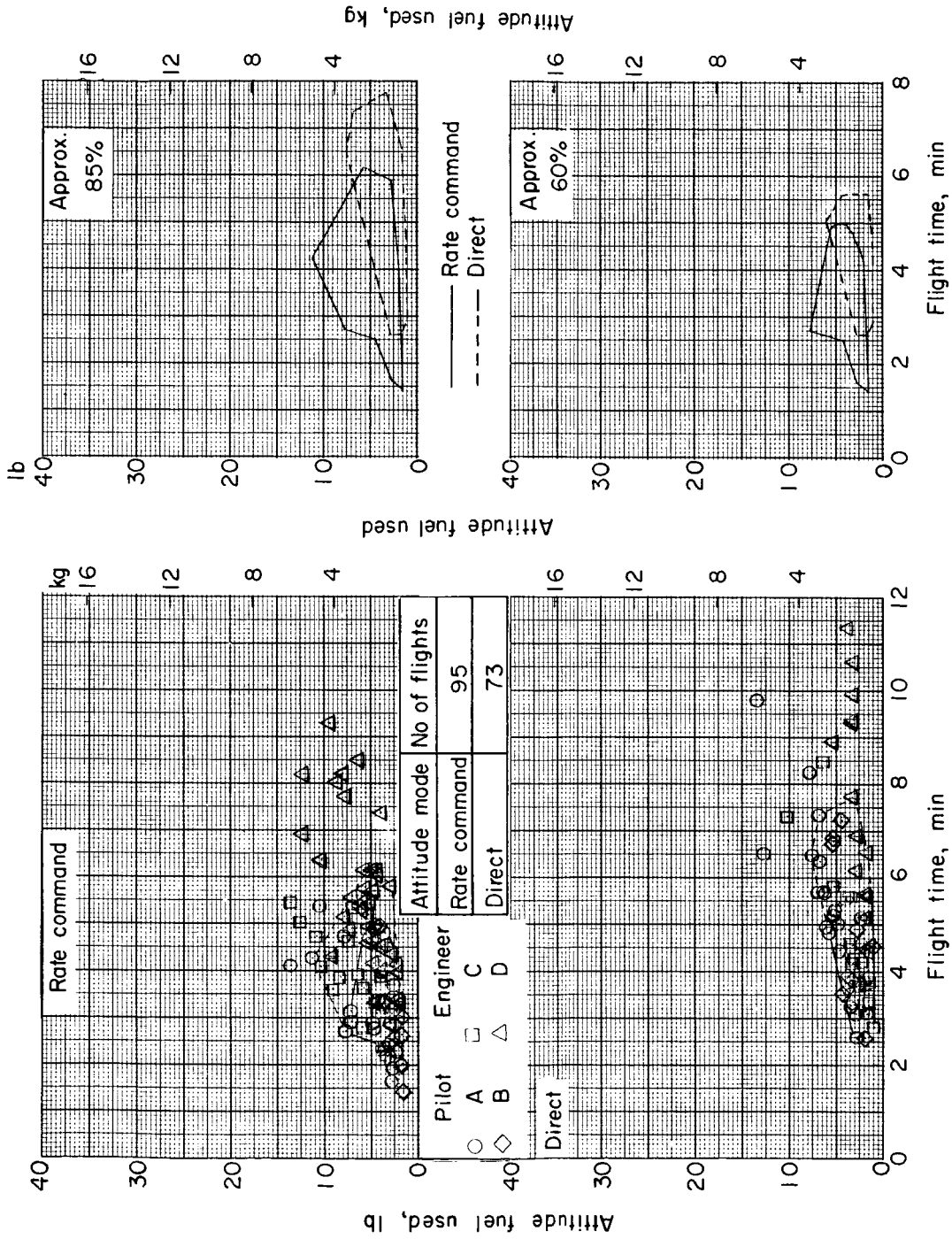
(a) Total fuel used.

Figure 11.- Fuel consumption as a function of flight time for four subjects using the rate-command and direct attitude control modes and a comparison of 60-percent and 85-percent data boundaries for the two control modes.



(b) Translation fuel used.

Figure 11.- Continued.

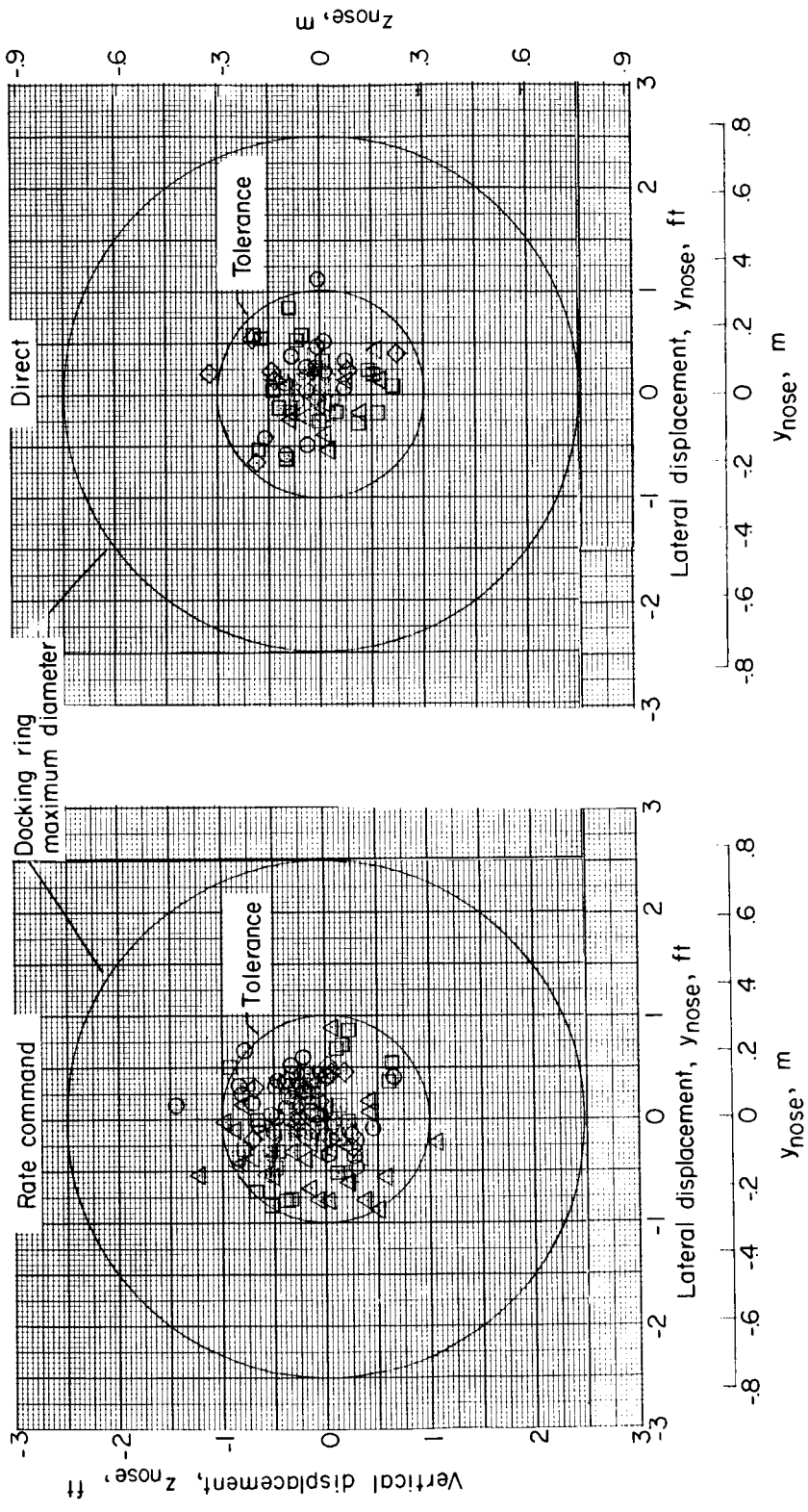


(c) Attitude fuel used.

Figure 11.- Concluded.

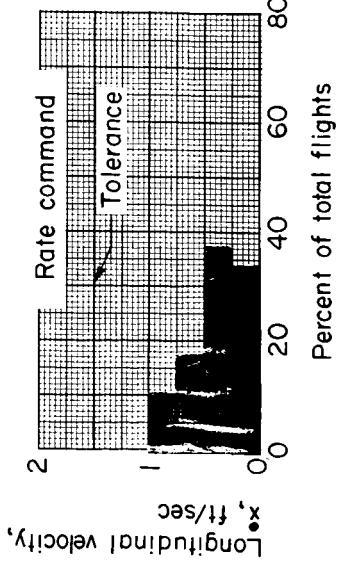
Mode	Total flights
Rate command	154
Direct	73

Pilot Engineer
 ○ □ △ ◇
 A B C D



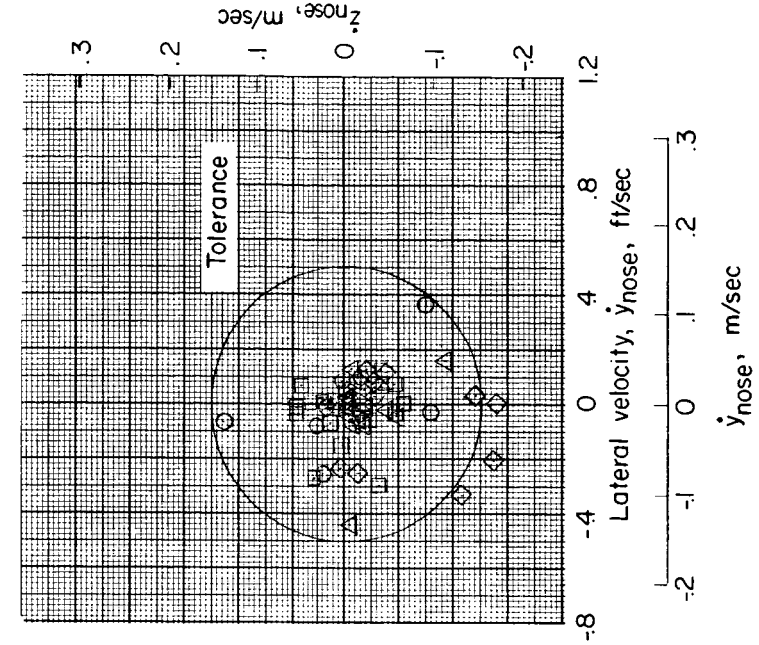
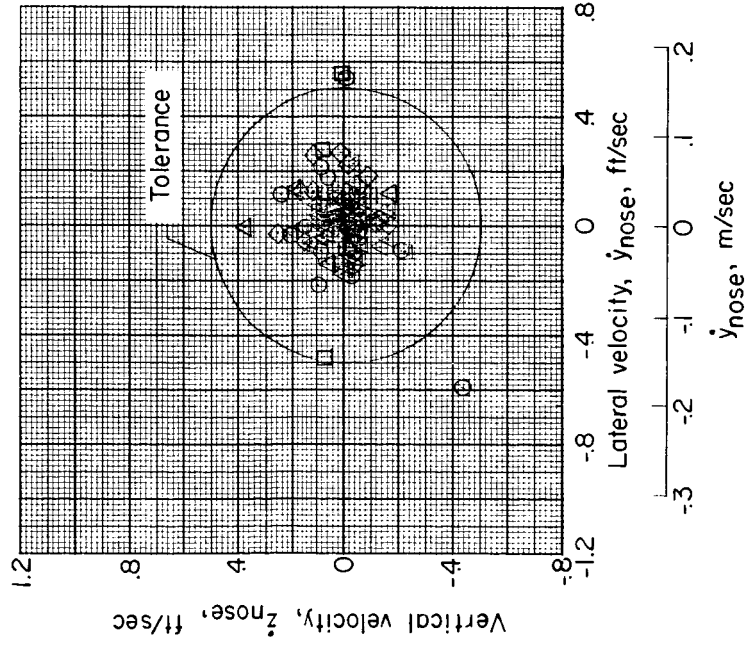
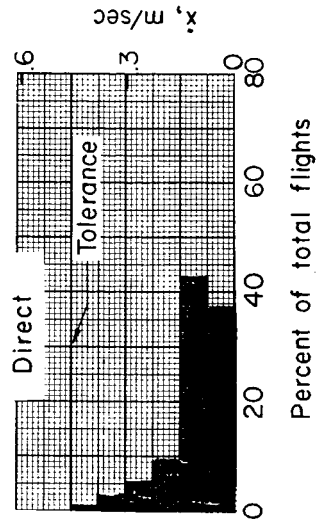
(a) Transverse displacements.

Figure 12.- Comparison of the terminal conditions obtained by four subjects using the rate-command and direct attitude control modes.



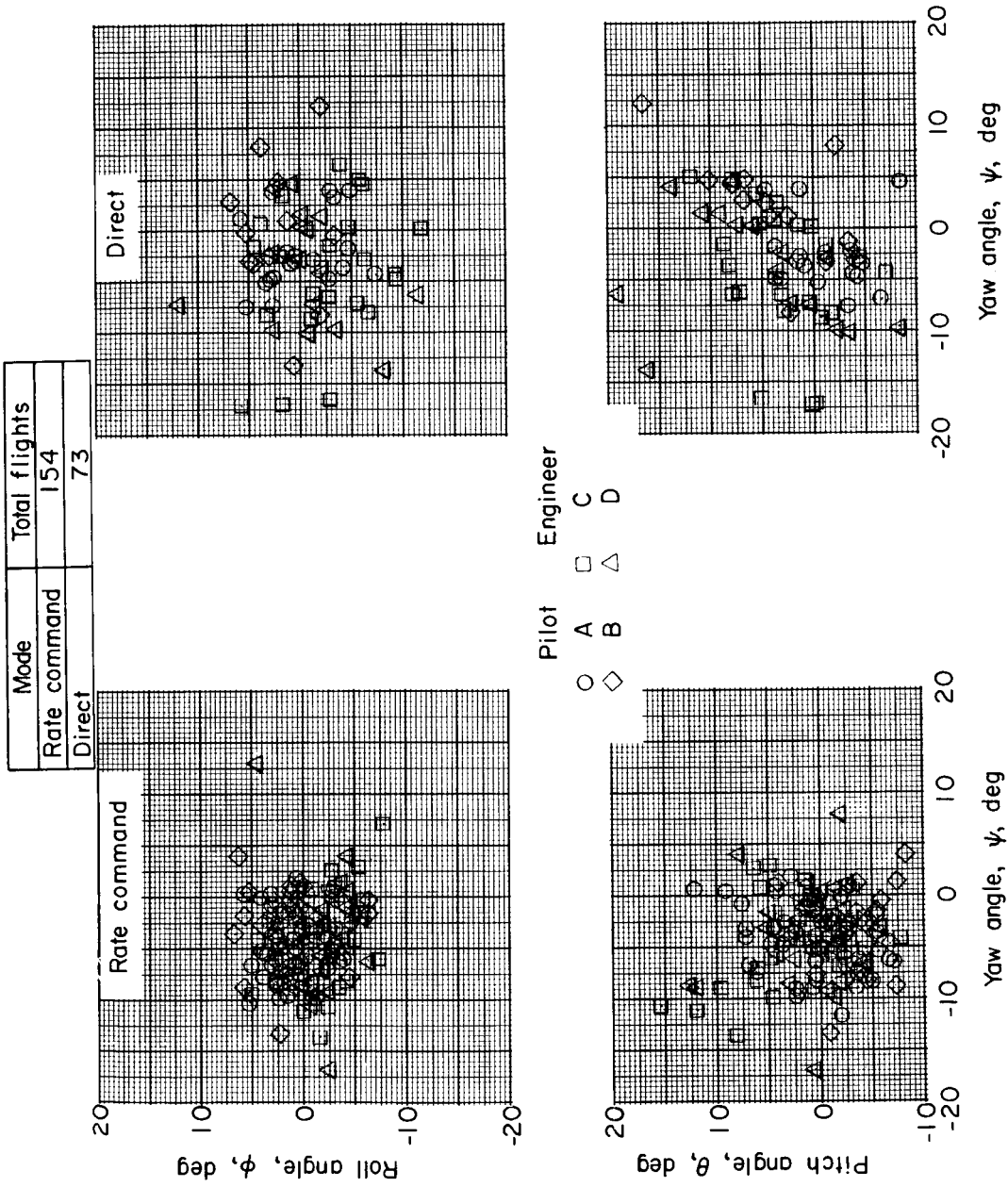
Mode	Total flights
Rate command	154
Direct	73

Pilot Engineer
 ○ A □ C
 ◇ B △ D



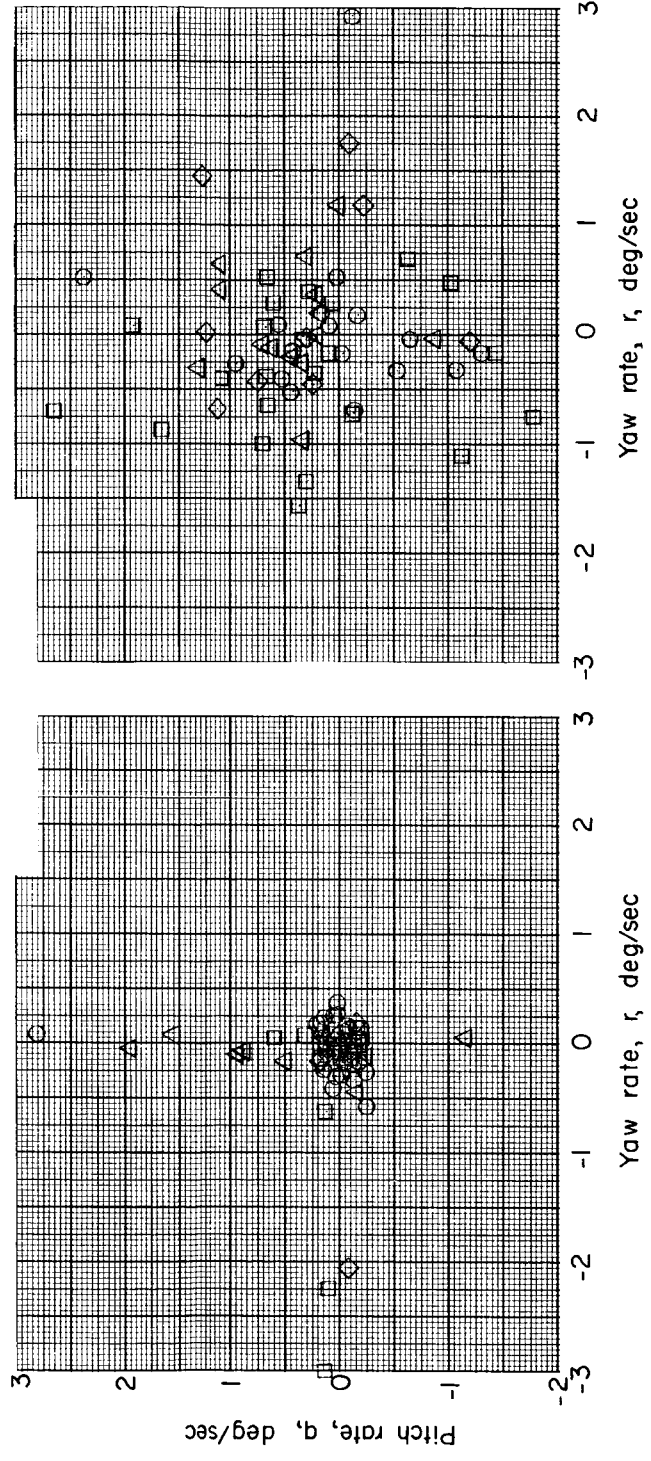
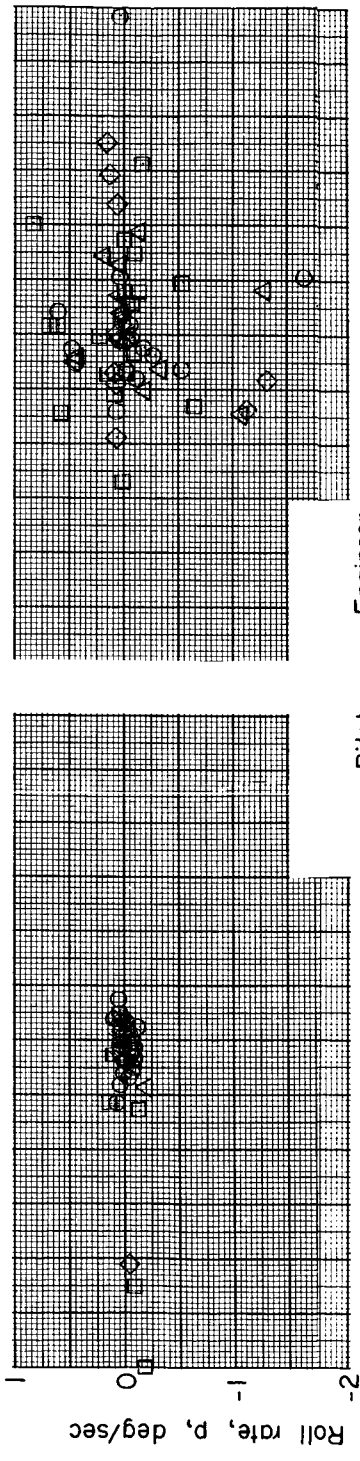
(b) Residual velocities.

Figure 12.- Continued.



(c) Angular misalignments (all tolerances, $\pm 10^\circ$).

Figure 12.- Continued.



(d) Gemini angular body rates (no tolerances specified).

Figure 12.- Concluded.

Pilot comments.

- A. _____
- B. Not responsive enough for translation corrections
- C. Worst case, attitudes not responsive enough - sluggish, not enough power to take care of cross coupling
- D. Good for close-in-maneuver and more desirable than A, but A more desirable at greater ranges
- E. _____
- F. Insufficient response

Display
Fully lighted target
Visual-aid bars attached

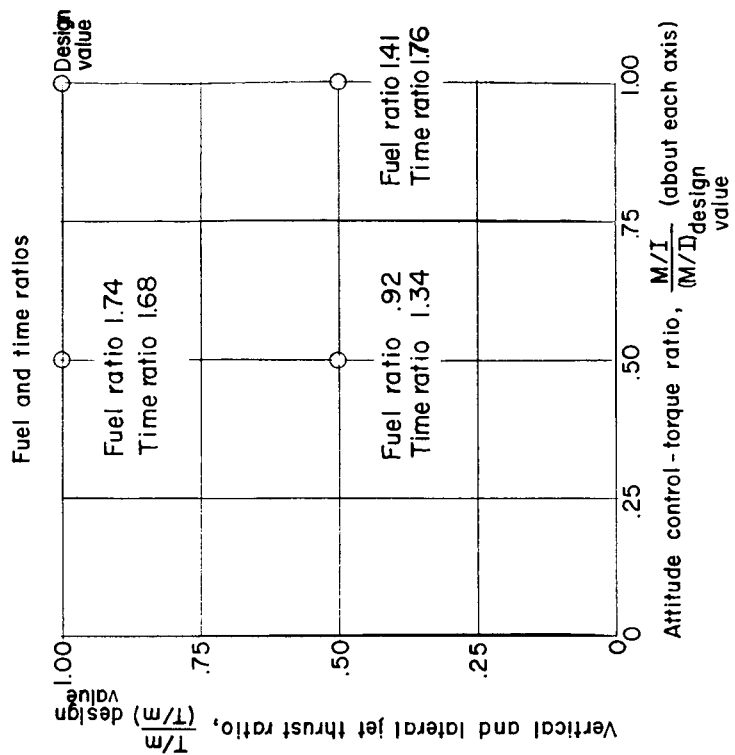
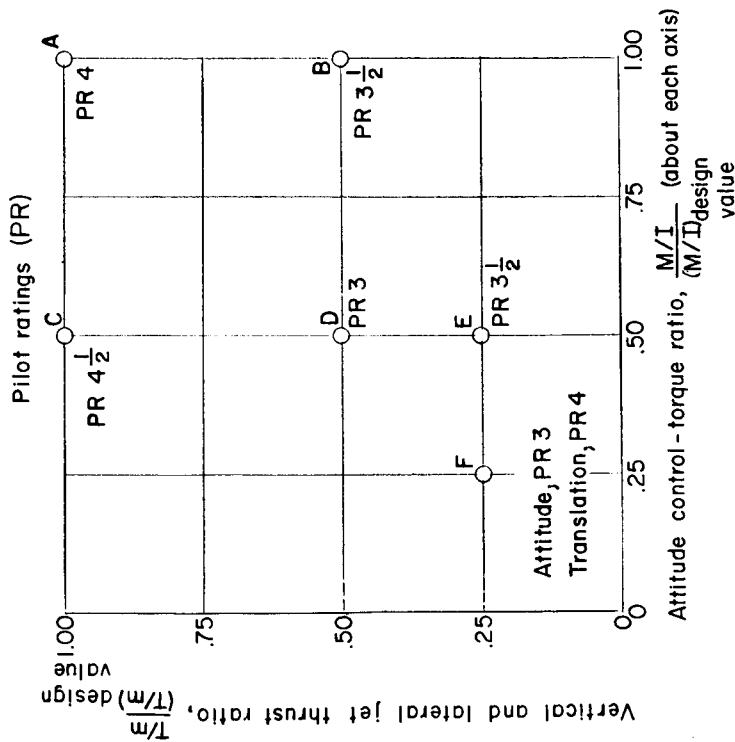


Figure 13.- Effect of varying translation thrust and attitude control torque from design condition on fuel consumed, flight time, and pilot opinion as determined by research pilot A using the direct attitude control mode. (Fuel ratio and time ratio normalized with respect to value obtained for design condition.)

Target lighting	Fully lit, no aids	Dark, no aids	Dark, with aids
Total flights	123	10	21

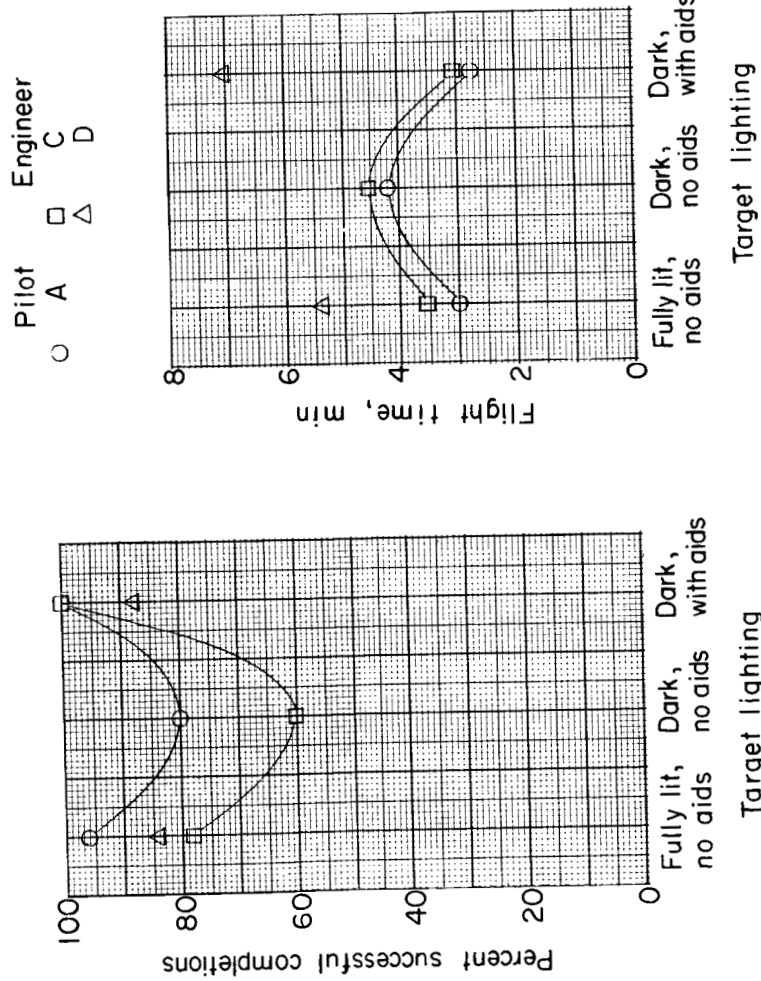


Figure 14.- Performance comparison for fully illuminated and darkside target configurations. (Rate-command attitude control mode used.)

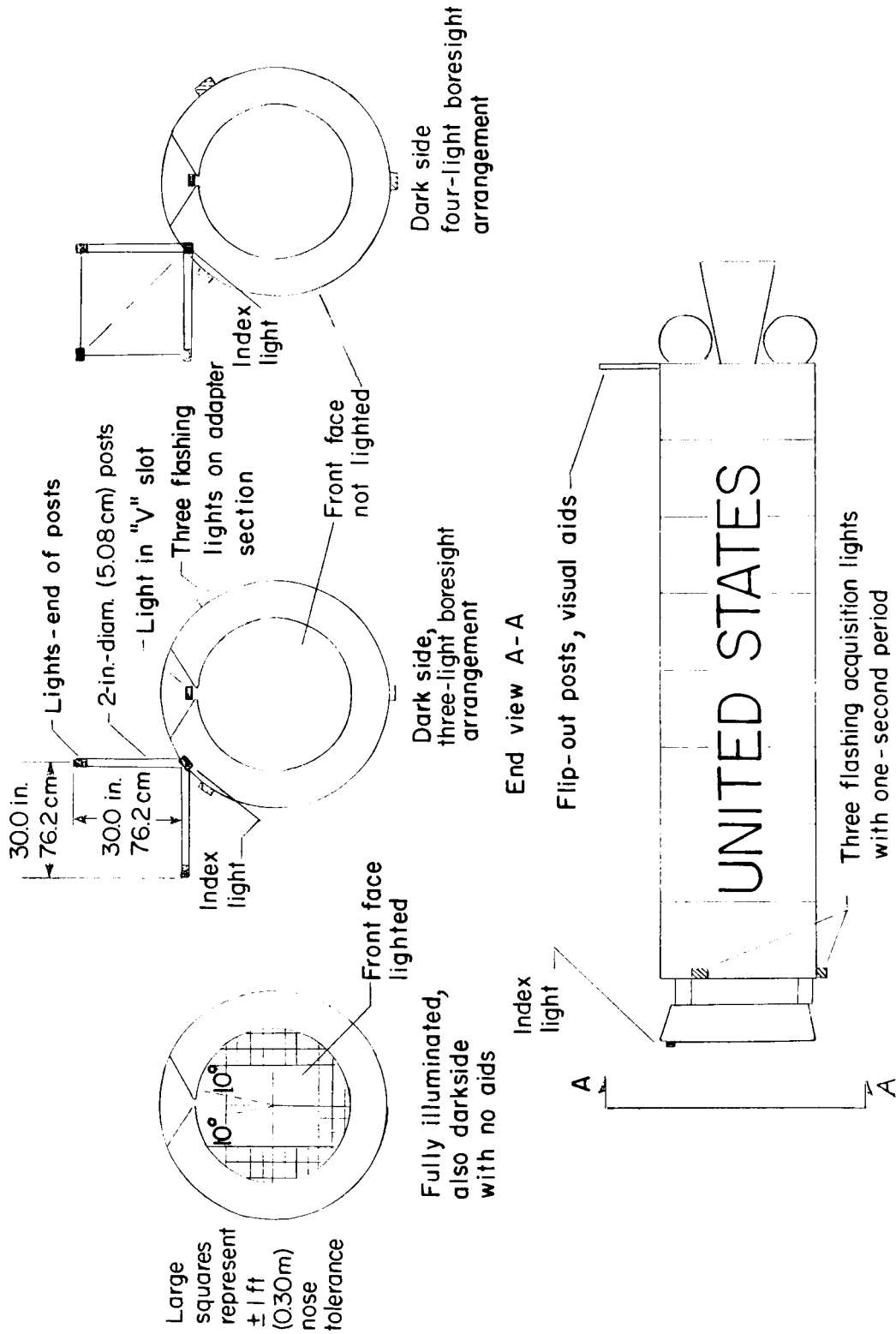
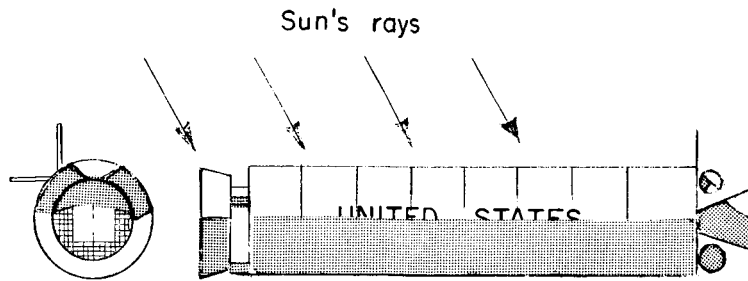


Figure 15.- Front face markings, light arrangements, and visual aids used on Agena target vehicle for daytime and darkside docking. (Note, index light is mounted where pilot's line of sight parallel to spacecraft center line intersects docking ring when vehicles are in perfect dock position.)

Partial illuminated target configuration



△ Pilots A and B
○ Engineers C and D

Target lighting	Full	Partial
Total flights	71	9
No. missed	13	1

Target lighting	Full	Partial
Total flights	18	7
No. missed	0	0

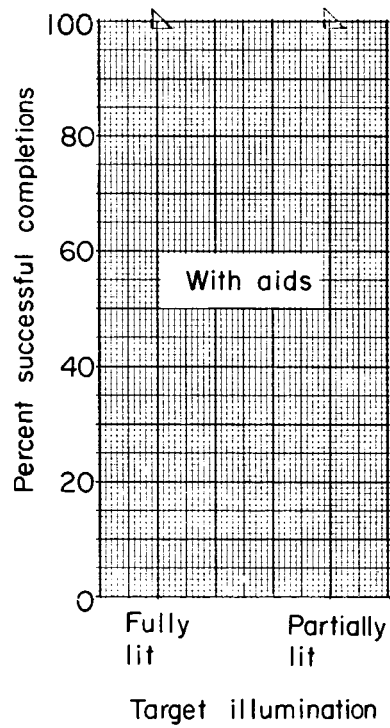
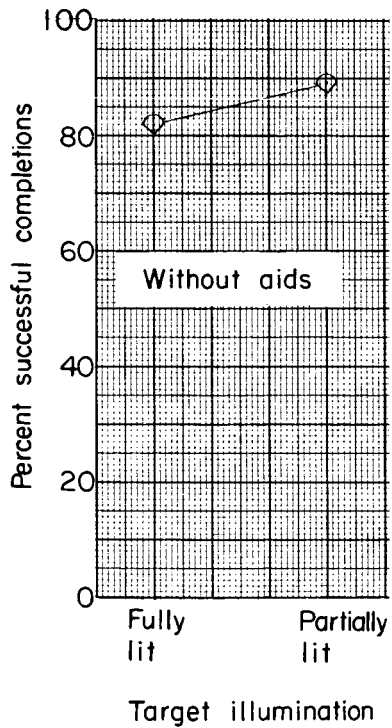
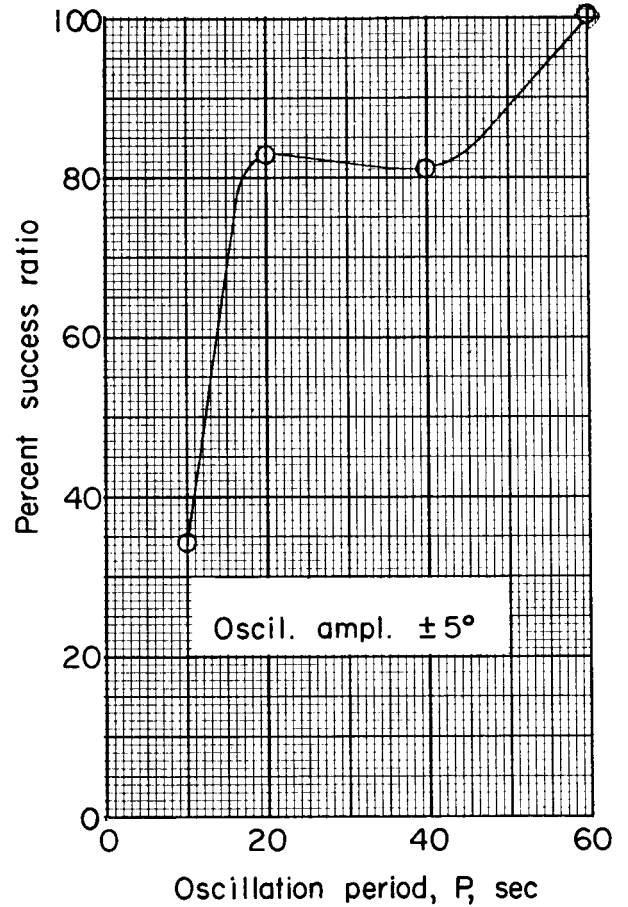
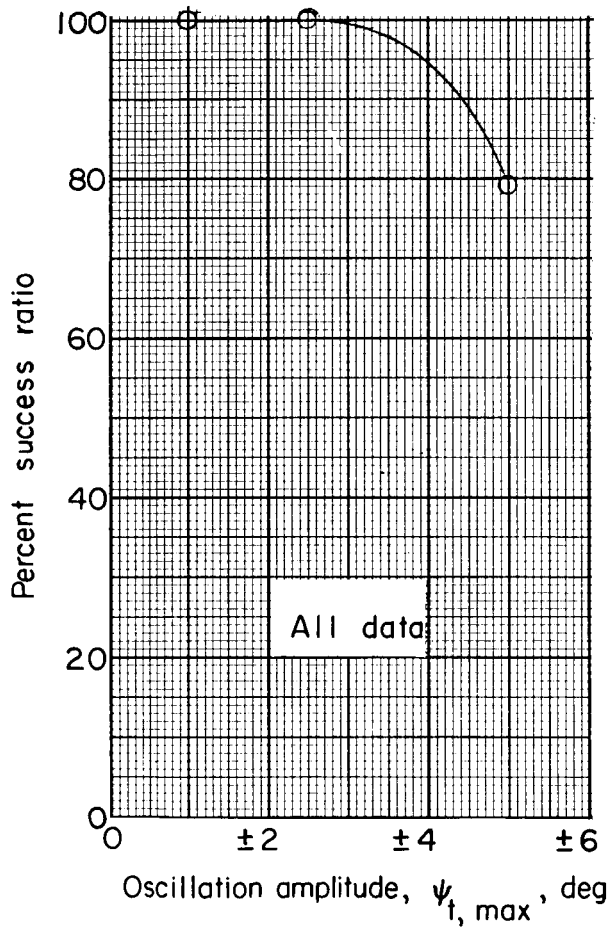


Figure 16.- Pilot's ability to perform successful docking with a fully and a partially illuminated target configuration.

Oscil. ampl	0°	±1°	±2.5°	±5°
No. of flights	16	10	15	56

Oscil. period	10	20	40	60
No. of flights	11	12	17	16

$$\text{Percent success ratio} = \frac{\text{Percent successful runs - target oscillating}}{\text{Percent successful runs - target not oscillating}}$$



(a) Amplitude effect (four pilots, both control modes, all periods).

(b) Effect of period (four pilots, both control modes, ±5° amplitude data only).

Figure 17.- Effect of amplitude and period of target yawing oscillation on percent successful completions ratio.

○ All data in .1 increments
 (4 pilots, both control modes,
 all amplitudes, all periods)

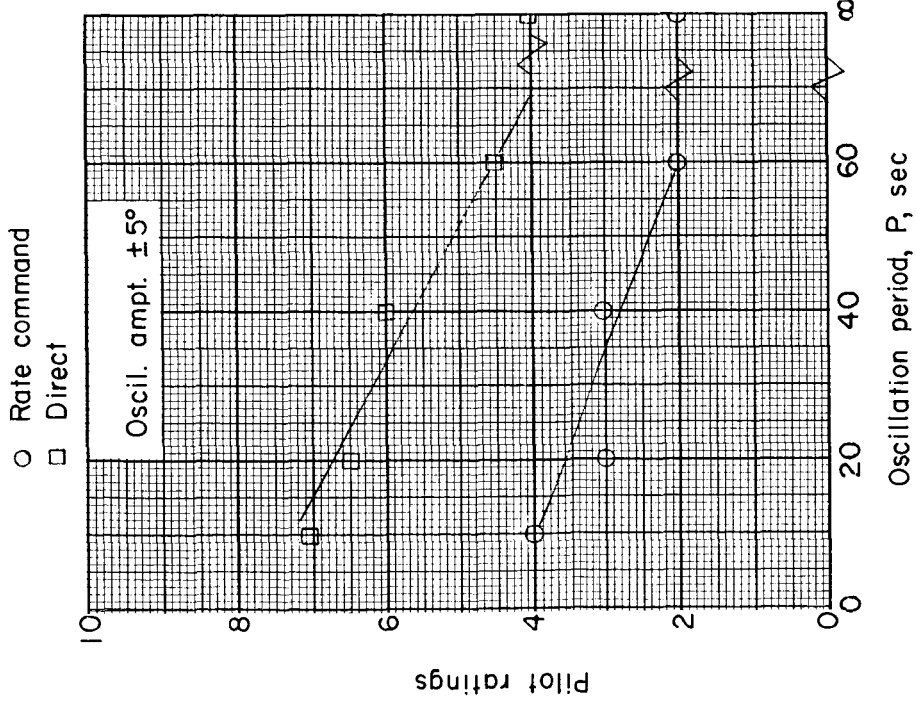
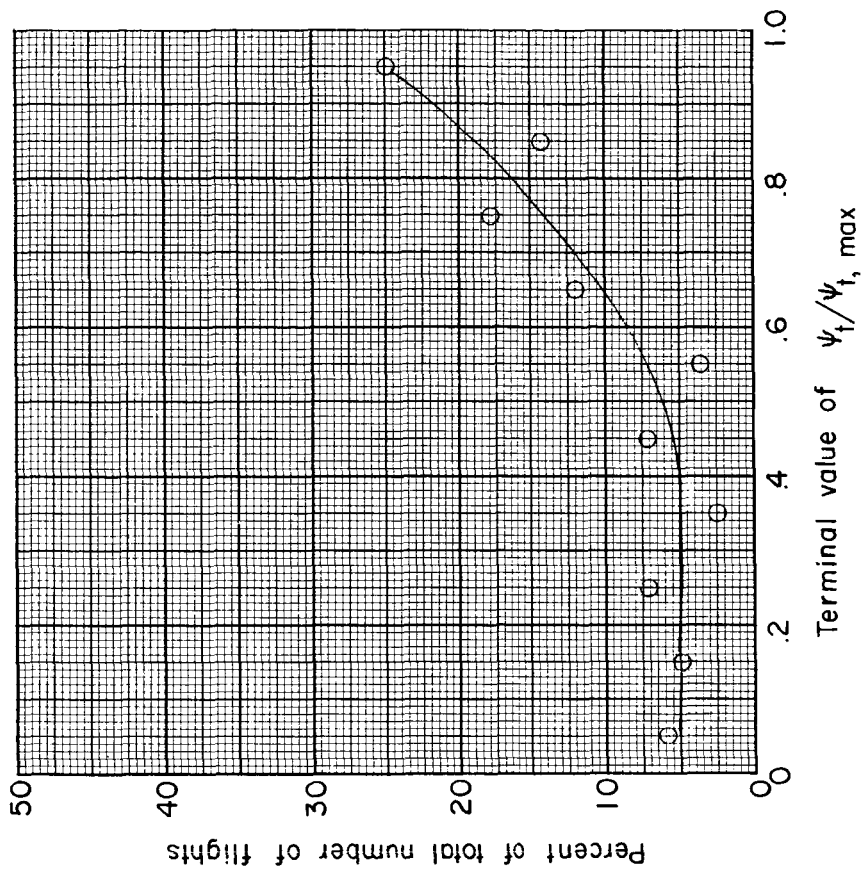
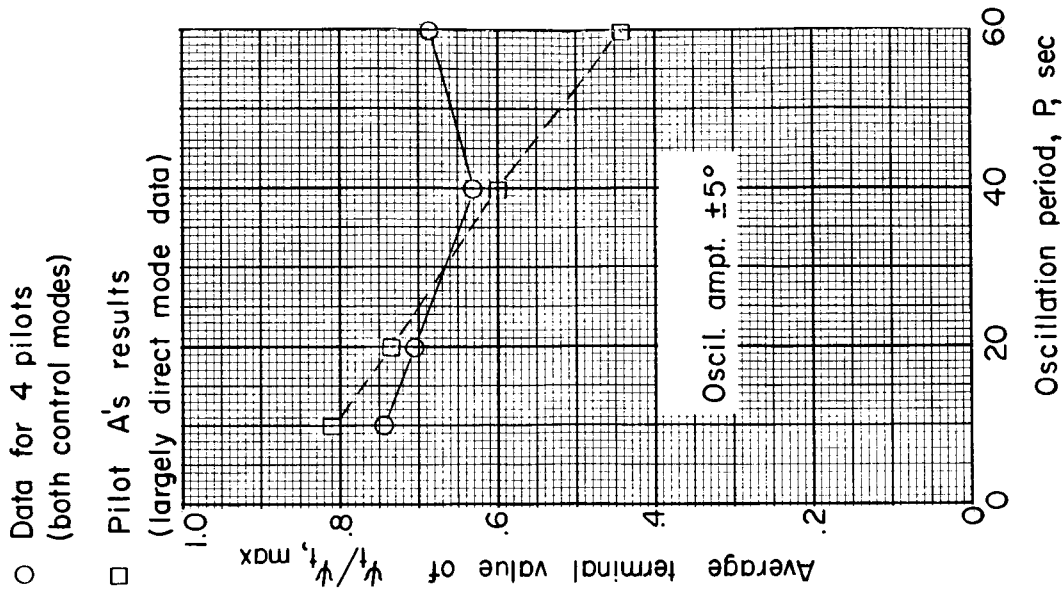


Figure 18.- Ratings by pilot A for single-degree-of-freedom oscillation in yaw tests. (Target fully illuminated with no visual aids; Gemini spacecraft paraglider configuration.) For rating schedule see table 1.

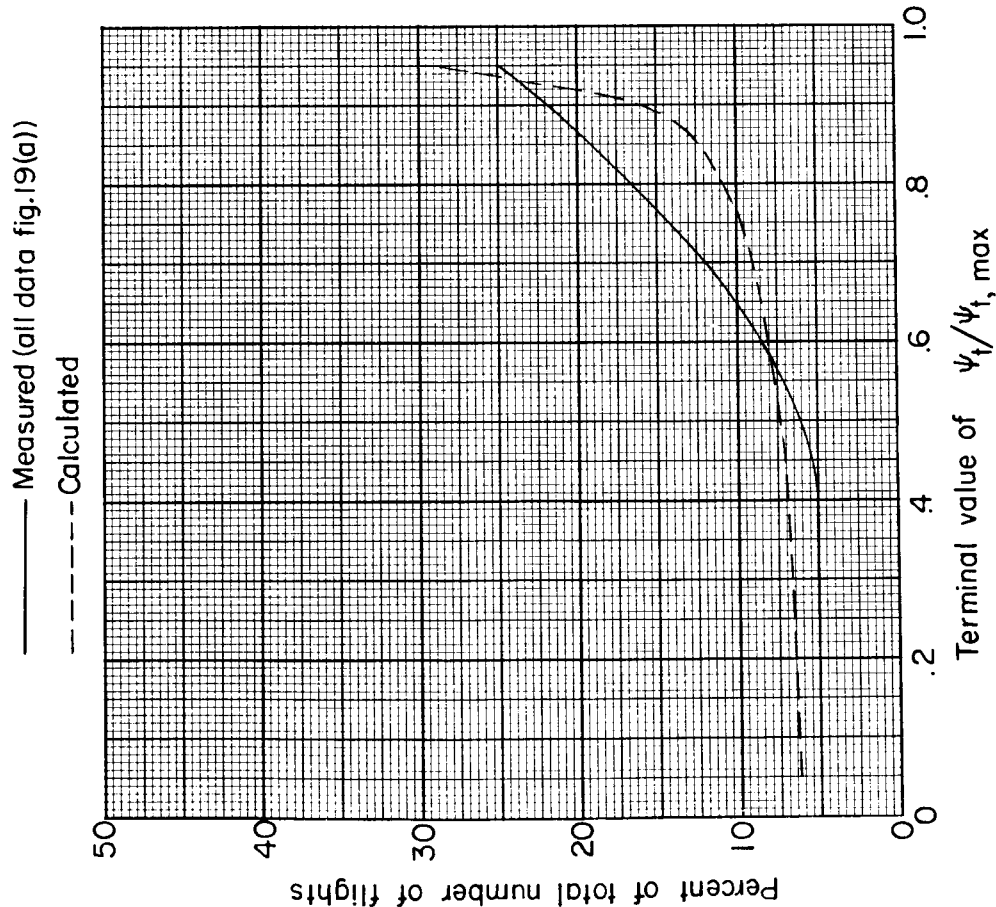


(a) Distribution curve.

Figure 19.- Distribution curves and effect of oscillation period on the terminal values for target yaw angle.



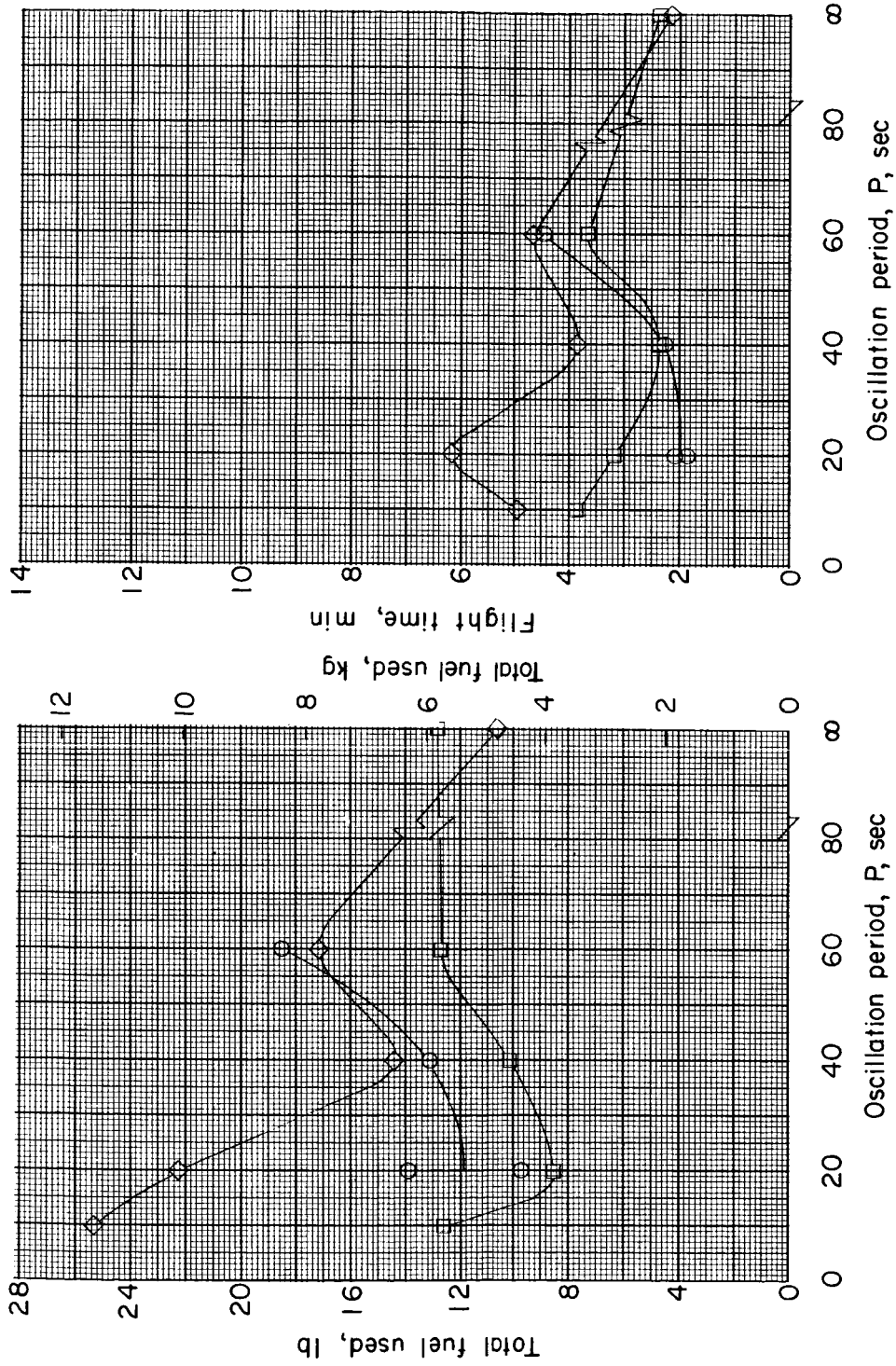
(c) Effect of period.



(b) Comparison of measured and calculated distribution curves.

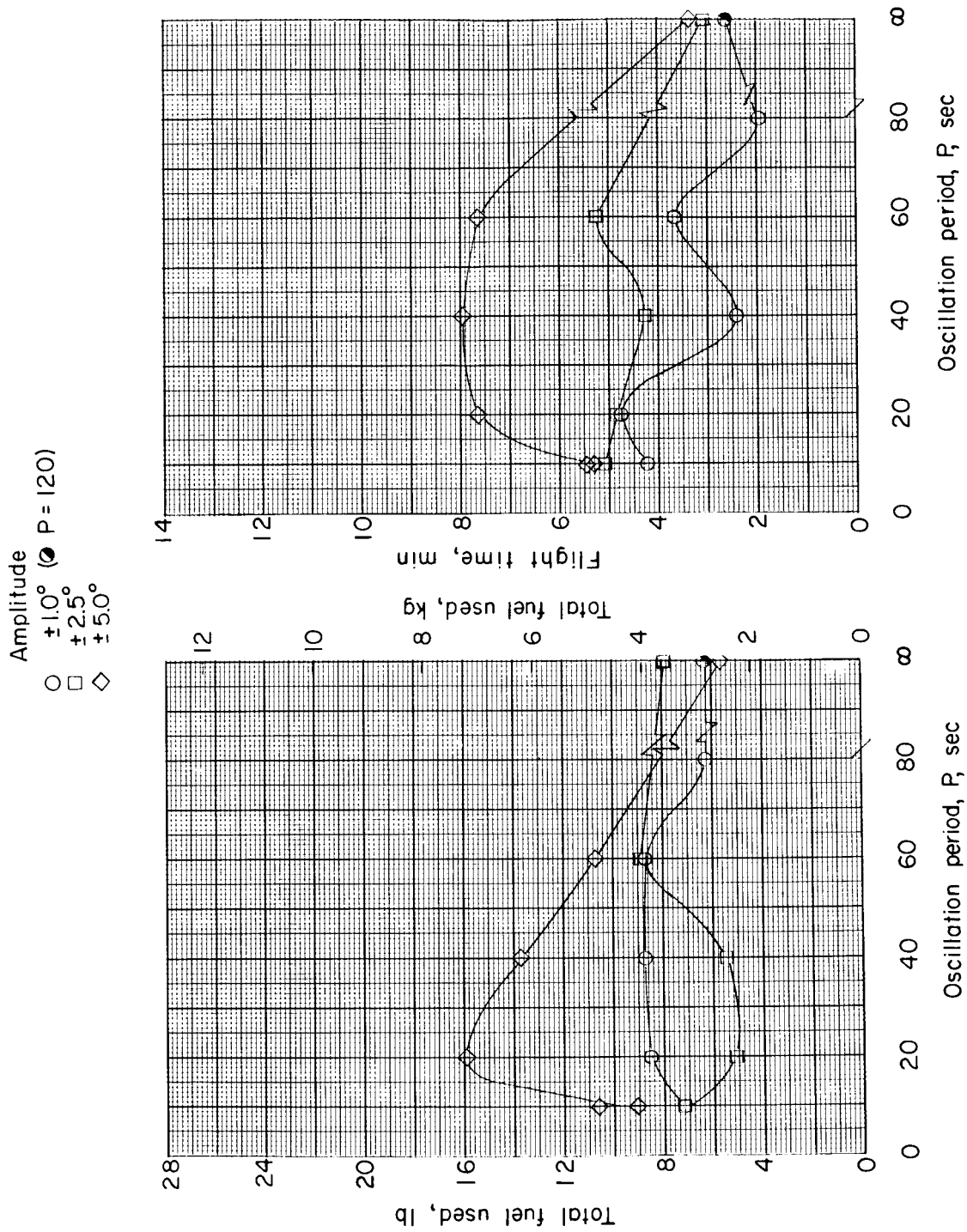
Figure 19.- Concluded.

Amplitude
 ○ ±1.0°
 □ ±2.5°
 ◇ ±5.0°



(a) Results of engineer C.

Figure 20.- Effect on total fuel and flight time of target yaw oscillation period and amplitude.



(b) Results of engineer D.

Figure 20.- Concluded.

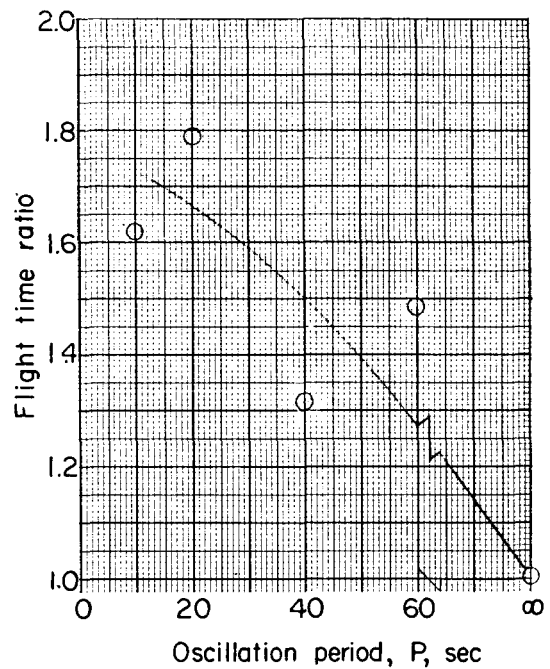
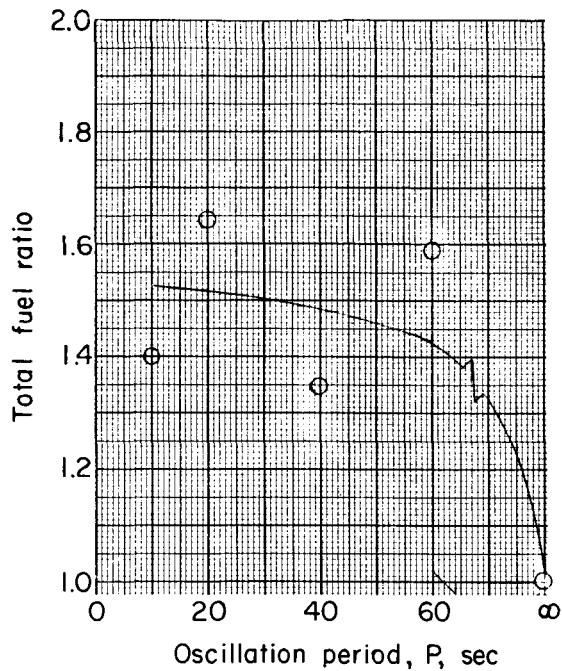


Figure 21.- Effect of oscillation period on three subjects' average total fuel and flight time ratios for $\pm 5^\circ$ amplitude data. (Results were normalized with respect to nonoscillating target. Both attitude control modes were included.)

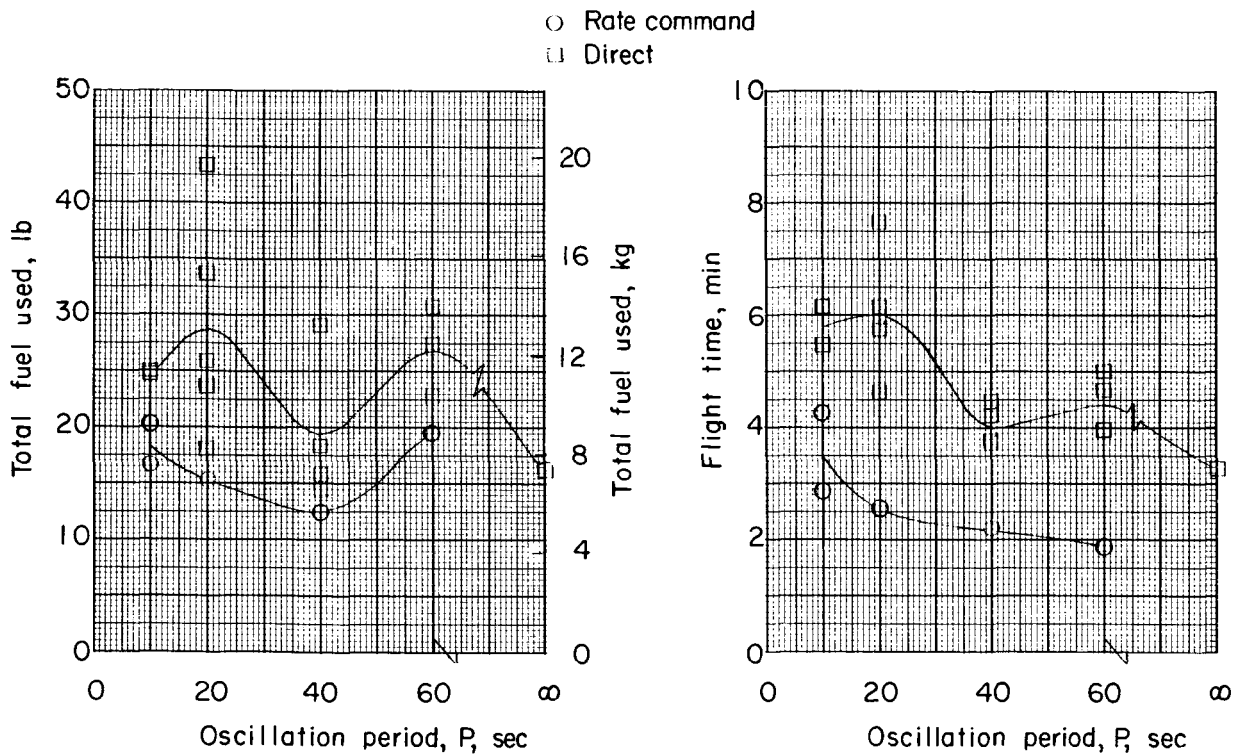


Figure 22.- Effect of attitude control mode on total fuel and flight time results obtained by pilot A for oscillation in yaw tests at an amplitude of $\pm 5^\circ$.

